DEEP TRANSFERABLE INTELLIGENCE FOR WEARABLE BIG DATA PATTERN DETECTION

by

Kiirthanaa Gangadharan

A Thesis

Submitted to the Faculty of Purdue University

In Partial Fulfillment of the Requirements for the degree of

Master of Science

Department of Electrical and Computer Engineering

Indianapolis, Indiana

August 2021

THE PURDUE UNIVERSITY GRADUATE SCHOOL
STATEMENT OF COMMITTEE APPROVAL

Dr. Qingxue Zhang, Chair

Department of Electrical and Computer Engineering

Dr. Brian King

Department of Electrical and Computer Engineering

Dr. Stanley Chien

Department of Electrical and Computer Engineering

Approved by:

Dr. Brian King

Dedicated to my friends and family who encourage and support me always and forever.

ACKNOWLEDGMENTS

I would like to express my sincere gratitude to my thesis advisor, Dr. Zhang, who made this work possible. His guidance and expertise have carried me through all stages of completing this research. I thank the committee members, Dr. King and Dr. Chien for having accepted to review my work. I also want to thank my academic advisor, Sherrie Tucker, for patiently addressing all my queries and helping me be on track since the beginning of my Graduate studies. And lastly, I am extremely grateful to my family, friends and classmates for their immense support and encouragement throughout this journey.

TABLE OF CONTENTS

LIST OF TABLES

LIST OF FIGURES

ABBREVIATIONS

x	Selected sensor/channel type
SwPAD	Sensor wise Physical Activity Detection
SCwPAD	Sensor and Channel wise Physical Activity Detection
SxPAD	Sensor - x - Physical Activity Detection
SCxPAD	Sensor and Channel - x - Physical Activity Detection
AX	Accelerometer-x channel
AY	Accelerometer-y channel
attr_ay	Accelerometer-y channel
AZ	Accelerometer-z channel
GX	Gyroscope-x channel
GY	Gyroscope-y channel
GZ	Gyroscope-z channel
cax	Accelerometer-x of chest sensor
cay	Accelerometer-y of chest sensor
caz	Accelerometer-z of chest sensor
cgx	Gyroscope-x of chest sensor
cgy	Gyroscope-y of chest sensor
cgz	Gyroscope-z of chest sensor
fax	Accelerometer-x of forearm sensor
fay	Accelerometer-y of forearm sensor
faz	Accelerometer-z of forearm sensor
fgx	Gyroscope-x of forearm sensor
fgy	Gyroscope-y of forearm sensor
fgz	Gyroscope-z of forearm sensor
hax	Accelerometer-x of head sensor
hay	Accelerometer-y of head sensor
haz	Accelerometer-z of head sensor
hgx	Gyroscope-x of head sensor

hgy	Gyroscope-y of head sensor
hgz	Gyroscope-z of head sensor
sax	Accelerometer-x of shin sensor
say	Accelerometer-y of shin sensor
saz	Accelerometer-z of shin sensor
sgx	Gyroscope-x of shin sensor
sgy	Gyroscope-y of shin sensor
sgz	Gyroscope-z of shin sensor
tax	Accelerometer-x of thigh sensor
tay	Accelerometer-y of thigh sensor
taz	Accelerometer-z of thigh sensor
tgx	Gyroscope-x of thigh sensor
tgy	Gyroscope-y of thigh sensor
tgz	Gyroscope-z of thigh sensor
uax	Accelerometer-x of upperarm sensor
uay	Accelerometer-y of upperarm sensor
uaz	Accelerometer-z of upperarm sensor
ugx	Gyroscope-x of upperarm sensor
ugy	Gyroscope-y of upperarm sensor
ugz	Gyroscope-z of upperarm sensor
wax	Accelerometer-x of waist sensor
way	Accelerometer-y of waist sensor
waz	Accelerometer-z of waist sensor
wgx	Gyroscope-x of waist sensor
wgy	Gyroscope-y of waist sensor
wgz	Gyroscope-z of waist sensor

ABSTRACT

Biomechanical Big Data is of great significance to precision health applications, among which we take special interest in Physical Activity Detection (PAD). In this study, we have performed extensive research on deep learning-based PAD from biomechanical big data, focusing on the challenges raised by the need for real-time edge inference. First, considering there are many places we can place the motion sensors, we have thoroughly compared and analyzed the location difference in terms of deep learning-based PAD performance. We have further compared the difference among six sensor channels (3-axis accelerometer and 3-axis gyroscope). Second, we have selected the optimal sensor and the optimal sensor channel, which can not only provide sensor usage suggestions but also enable ultra-low-power application on the edge. Third, we have investigated innovative methods to minimize the training effort of the deep learning model, leveraging the transfer learning strategy. More specifically, we propose to pre-train a transferable deep learning model using the data from other subjects and then fine-tune the model using limited data from the target-user. In such a way, we have found that, for single-channel case, the transfer learning can effectively increase the deep model performance even when the fine-tuning effort is very small. This research, demonstrated by comprehensive experimental evaluation, has shown the potential of ultra-low-power PAD with minimized sensor stream, and minimized training effort.

1. INTRODUCTION

The field of Physical Activity Detection (PAD) has a wide range of applications such as health analysis, mobility tracking, and security systems. The advancement of the Internet of Things enables easy access to affordable wearable devices [1] [2] [3] that perform a mass collection of data from their inbuilt inertial sensors. The devices attached to a person collect PAD data through Sensor signals from an accelerometer, heart rate monitors, thermometers, and gyroscope [4]. It contains information on types of sensors used, signal sampling rates, length of times series of the activity performed, and feature processing techniques. The data captured from the sensor devices are recognized using different Machine learning techniques. These models are used to recognize better, classify, cluster, and predict human activities and help in further decision making.

There are previous studies reported using machine learning [5] for PAD tasks. For example, the support vector machine [6] [7] has been developed for human activity analysis. Other classifier methods [8] [9] like the Random Forest, Naive Bayes, decision trees have also been described for analysis. However, as these methods usually require manual feature engineering, the efforts for feature design and the generalization ability of the models may be constrained. Thus, we propose to study deep learning methods for PAD tasks.

Deep learning [10] is an essential type of ML algorithm that uses statistics and predictive modeling in data analysis. It involves the collection of data, analyzing, and interpreting large amounts of data. It is very beneficial due to the following reasons. First, the deep learning architecture is adaptable to new problems that may arise in the future. In this method, the features are automatically deduced and optimally tuned for the desired outcome. Second, we can perform heavy parallel training that utilizes large volumes of data using GPUs.

There are deep learning [11] [12] [13] - based PAD methods reported. These have shown the potential of automatic feature learning and inference using deep neural network models. Nevertheless, the comprehensive analysis of different sensor locations on the body is still limited. Therefore, we propose first to investigate the difference among these sensor locations using deep learning. This study will help minimize the need for sensor streams for effective PAD tasks. Further, we are interested in minimizing training effort for the deep

learning models, meaning that we propose to leverage transfer learning to learn shareable deep learning models that can be applied to the target user for quicker adaptation.

The main benefit of transfer learning [14] [15] [16] is that we need fewer data to train the neural network, which is particularly important because training for deep learning algorithms is expensive in terms of both time and effort. Thus, it is used best in places where it is challenging to find enough labeled data for training. Without transfer learning, we will have to use significantly larger datasets to get results. Furthermore, since transfer learning is performed by leveraging knowledge obtained from prior training methods, it is expected to speed up the training process significantly.

Our major contributions are summarized below:

First, considering there are many places we can place the motion sensors, we have thoroughly compared and analyzed the location difference in terms of deep learning-based PAD performance. Then, we have further compared the difference among six sensor channels (3-axis accelerometer and 3-axis gyroscope).

Second, we have selected the optimal sensor and the optimal sensor channel, which can not only provide sensor usage suggestions but also enable ultra-low-power application on the edge.

Third, we have investigated innovative methods to minimize the training effort of the deep learning model, leveraging the transfer learning strategy. More specifically, we propose to pre-train a transferable deep learning model using the data from other subjects and then fine-tune the model using limited data from the target user.

We have found that, for the single-channel case, using the transfer learning method can effectively increase the deep model performance even when the fine-tuning effort is minimal. This research, demonstrated by comprehensive experimental evaluation, has shown the potential of ultra-low-power PAD with minimized sensor stream, and minimized training effort.

2. OVERVIEW OF DATA AND METHODS

2.1 Overview of Data and Methods

The Real-World Dataset [17] created by the University of Mannheim — Research Group Data and Web Science is selected for this study. In total, the six activity classes are: climbing downstairs, climbing upstairs, jumping, lying, running/jogging, and walking. The smart devices to record sensor data were attached to the 15 Subjects in 7 different body regions: chest, forearm, head, shin, thigh, upper arm, and waist. These subjects performed each activity for approximately 10 minutes (except for jumping, approx. 2 minutes). [18] Both accelerometer and gyroscope data are used in the study.

As shown in Fig.2.1, each method involves five basic operations. Data pre-processing, evaluation using CNN model [19], generate deep learning curves and classification report and arrive at a conclusion based on accuracy comparison of different methods. Initially, we perform few preliminary operations on raw data to prepare it for mainstream data analysis. Each channel from each activity of the whole dataset is first visualized using matplotlib. Fig. 2.2 shows an example of the sample visualization of two activities – running and climbing up performed by Subject 8. It contains all the six different channel types – tri-axial accelerometer and tri-axial gyroscope values. The activity plot of the dataset based on different features is discussed in length under Chapter 2. Finally, the total number of instances is split into 80% training data and 20% test data for model classification, which will be discussed in detail under Chapter 3.

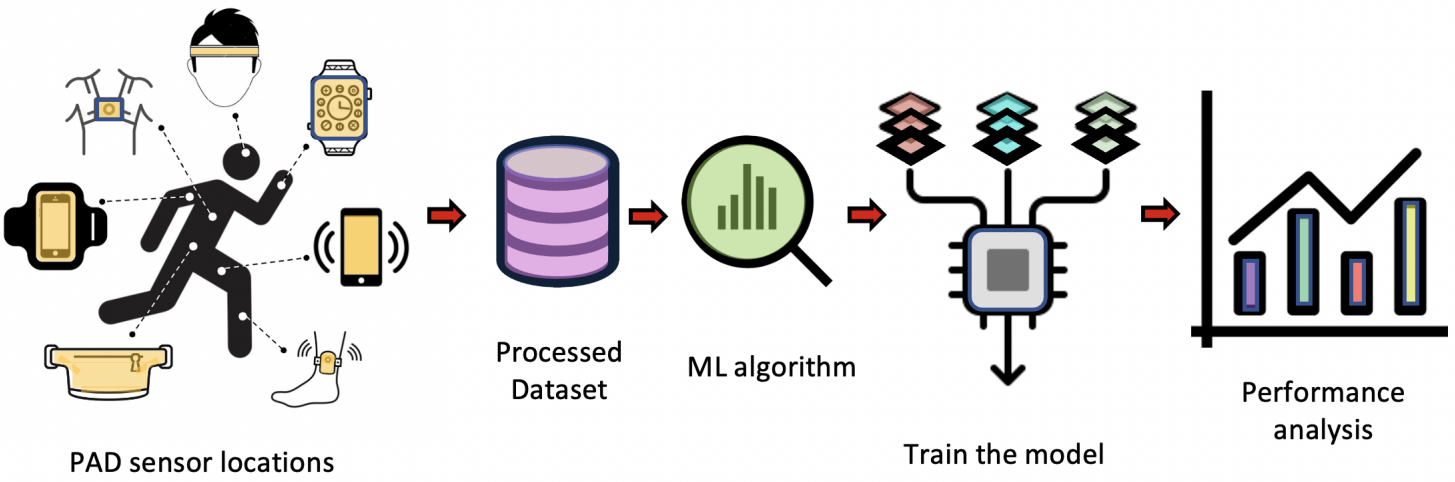

Figure 2.1. The application scenario of deep learning implementation using biomechanical big data. PAD: Physical Activity Detection, ML: Machine Learning

Once the data is processed, it is ready for analysis. We analyze the PAD dataset in four methods as follows. Sensor-wise Physical Activity Detection (SwPAD) method, Sensor and Channel wise Physical Activity Detection (SCwPAD) method, Sensor - x Physical Activity Detection (SxPAD) method, and Sensor and Channel - x Physical Activity Detection (SCxPAD) method where x is optimal selection based on former analysis. In the first two methods, the dataset is split based on the type of sensor, and the channel is trained using the [20] CNN model to determine the best sensor location and channel type derived from the results of the prediction model to be used for further study. The step-by-step procedure of the process is discussed in length under Chapter 3 and Chapter 4, respectively. Then, the SxPAD and SCxPAD methods are implemented using results from the former methods. Direct learning and transfer learning methodology are applied to these techniques, with datasets generated using sensor locations and channels selected from the previous method. A detailed explanation is given in Chapter 5 and Chapter 6. Finally, Chapter 7 discusses the output generated from all four methods, accuracy comparison, and much in a concise manner.

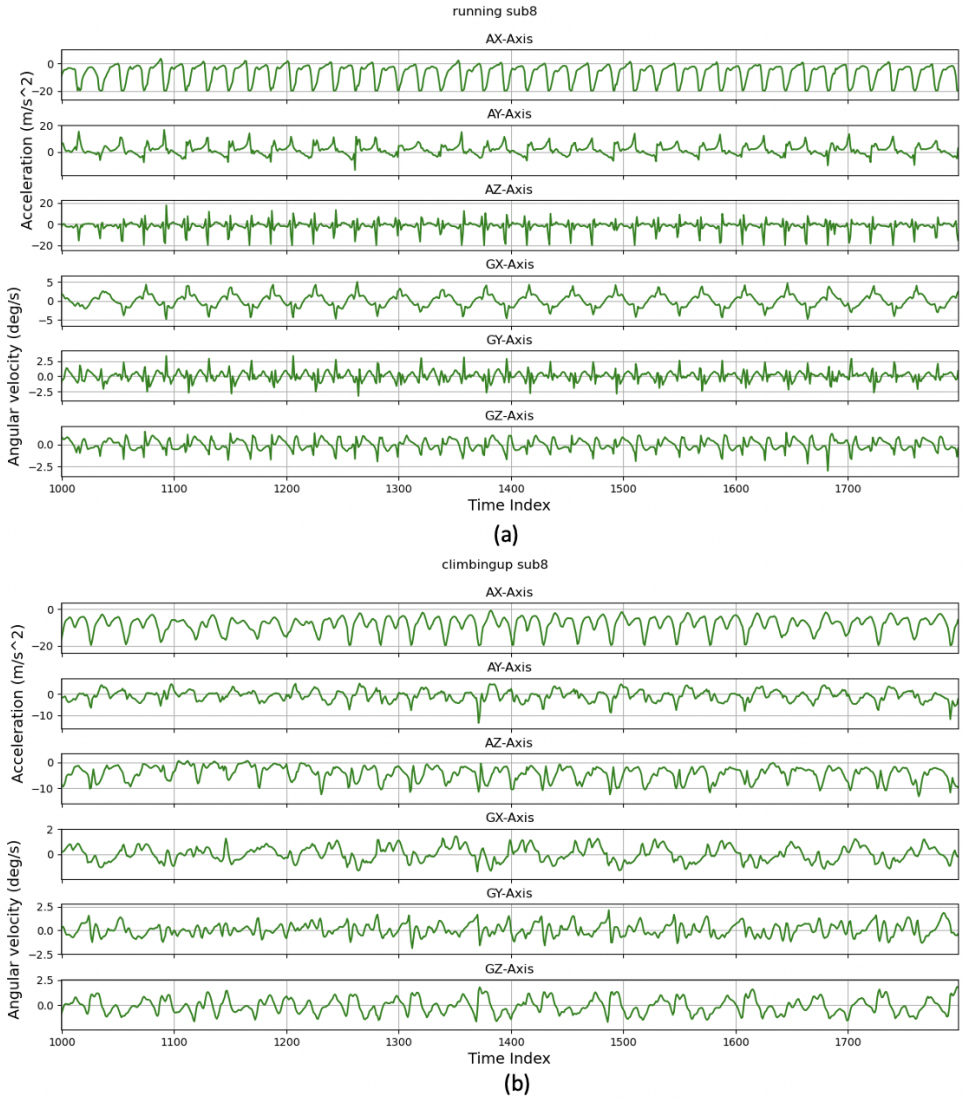

Figure 2.2. The visualization plot of selected samples with tri-axial accelerometer and gyroscope data from two different activities (a). Running and (b). Climbing up of Subject 8 in the real-world dataset.

In this chapter, we further discuss the activity plot of PAD data based on different features. As we know, the PAD dataset is a large dataset with a copious collection of sensor activity. First, let us list the different features in which the dataset can be categorized for visualization: Based on Subject id - the dataset comprises 15 different subjects. Based on activity – we have chosen the following six activities for our study. Climbing up, climbing down, jumping, lying, running, and walking. Based on sensor location – Chest, forearm, head, shin, thigh, upper arm, and waist. Based on channel type – accelerometer X, accelerometer Y, accelerometer Z, gyroscope X, gyroscope Y, and gyroscope Z.

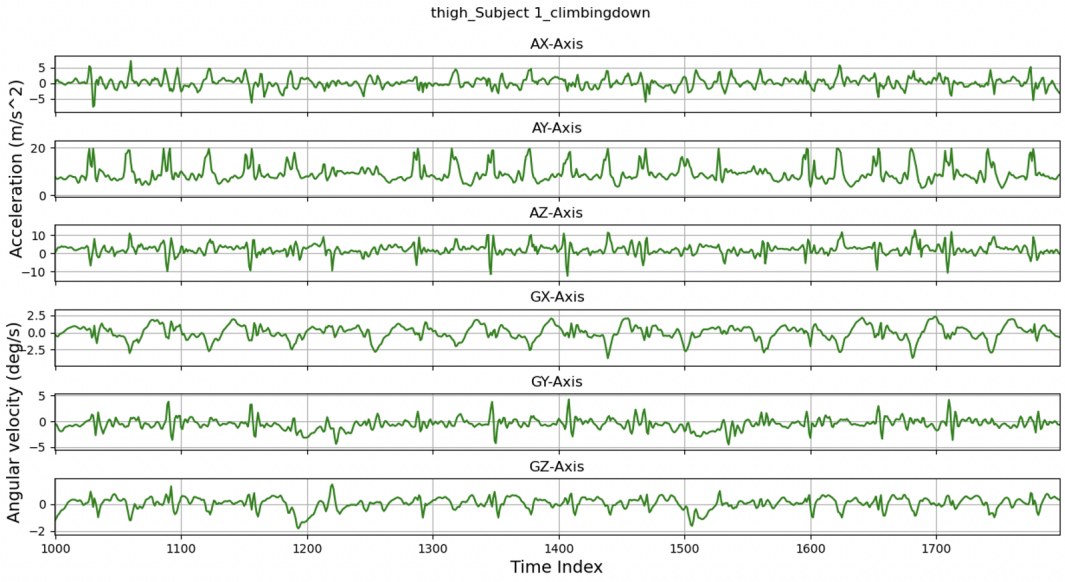

Figure 2.3. Visualization plot of 4-trial data of Climbing down activity with six-axis from Thigh sensor location belonging to Subject 1.

Representation of tri-axial sensor data with different activity and subjects are shown in the figures to follow. Data is represented as segments, and each segment is called a trial which consists of 200 samples. Therefore, Fig. 2.3 contains 800 samples of data as it is a 4-trial visualization of climbing down activity captured from thigh sensor location.

The seven plots in Fig. 2.4 represent climbing up activity captured from each of the seven sensor locations. Thus, we can compare the trace of these seven sensors and how each channel generates different waveforms.

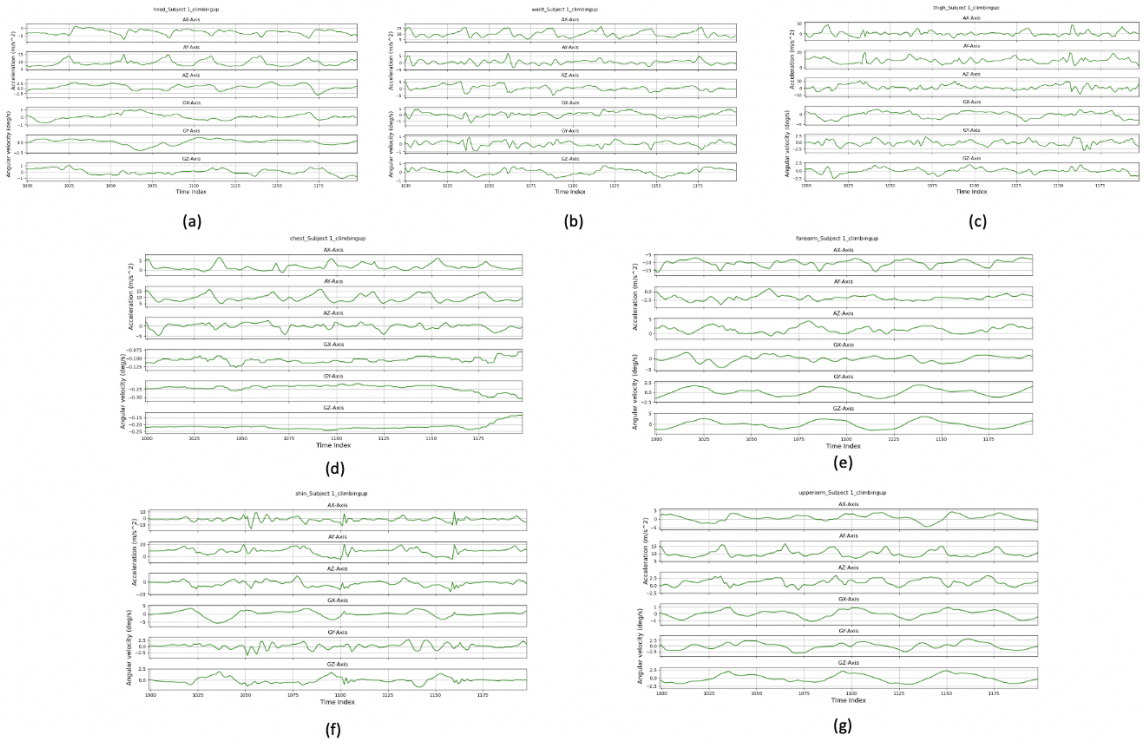

Figure 2.4. Visualization plot of 1-trial data of Climbing up activity with six-axis belonging to Subject 1 from all seven-sensor locations. (a). Head sensor, (b). Waist sensor, (c). Thigh sensor, (d). Chest sensor, (e). Forearm sensor, (f) Shin sensor, and (g). Upperarm sensor.

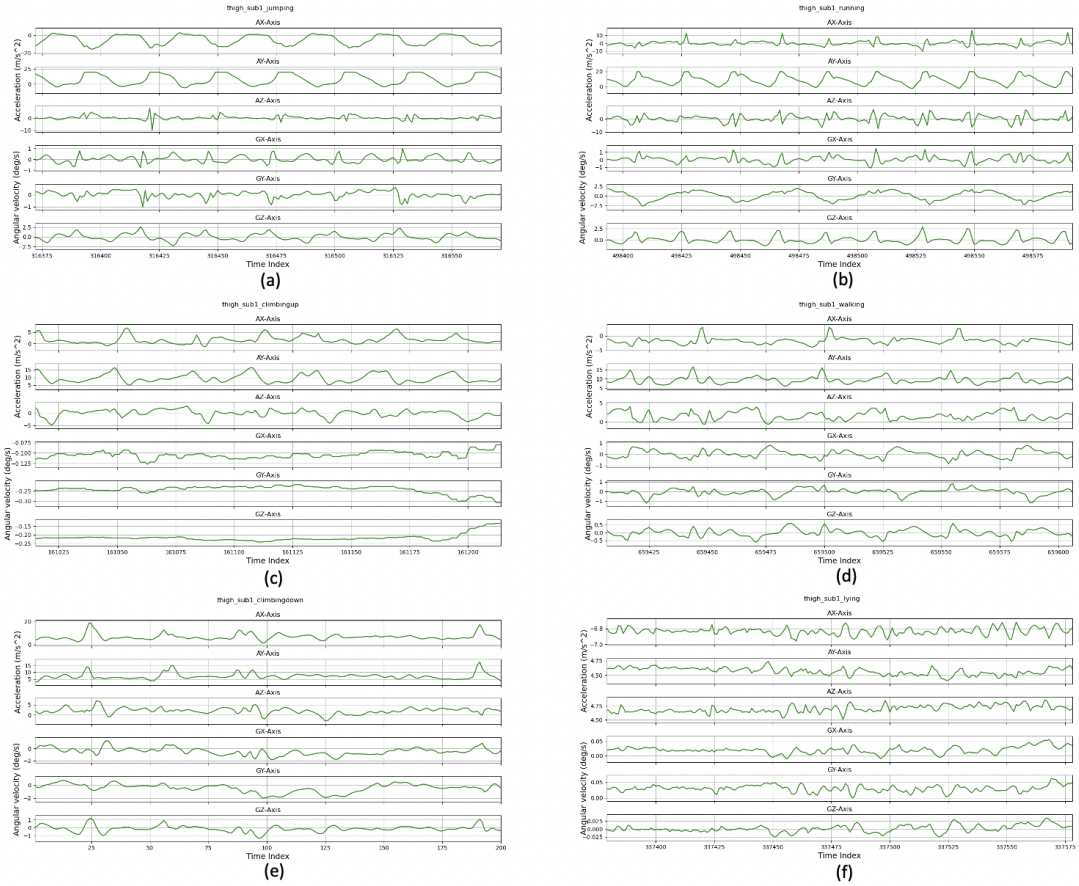

Figure 2.5. Visualization plot of 1-trial data from Thigh sensor location with six axes of all six activities belonging to Subject 1. (a). Jumping, (b). Running, (c). Climbing up, (d). Walking, (e). Climbing down, (f) Lying.

The difference in the pattern by different activity is shown in Fig. 2.5, where each plot depicts one kind of activity performed by the same user from the exact sensor location. Finally, Fig. 2.6 and Fig. 2.7 are visualization plots of one kind of activity belonging to all subjects. By generating these plots, we realize the trend of each channel with respect to their activity type and sensor type, which will be used for analysis in training the classification model in further study.

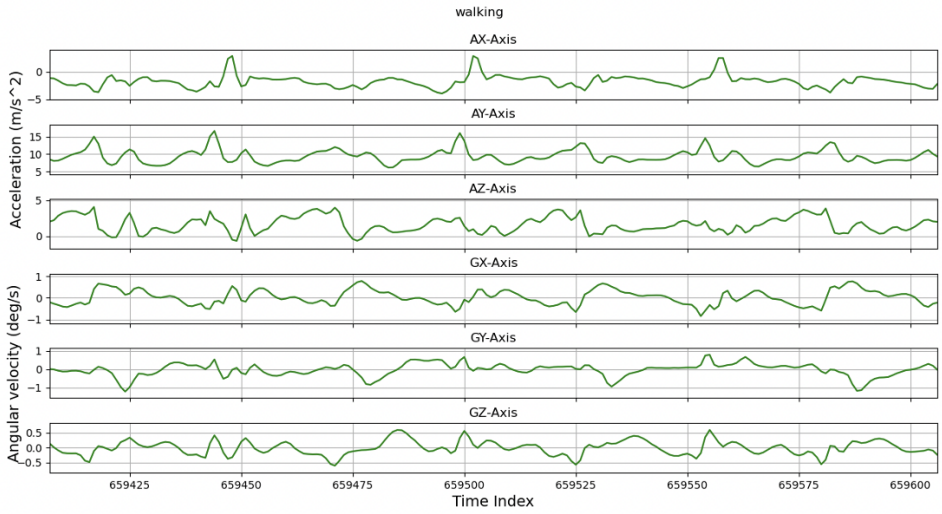

Figure 2.6. Visualization plot of 1-trial data of Walking activity with six axes belonging to all subjects.

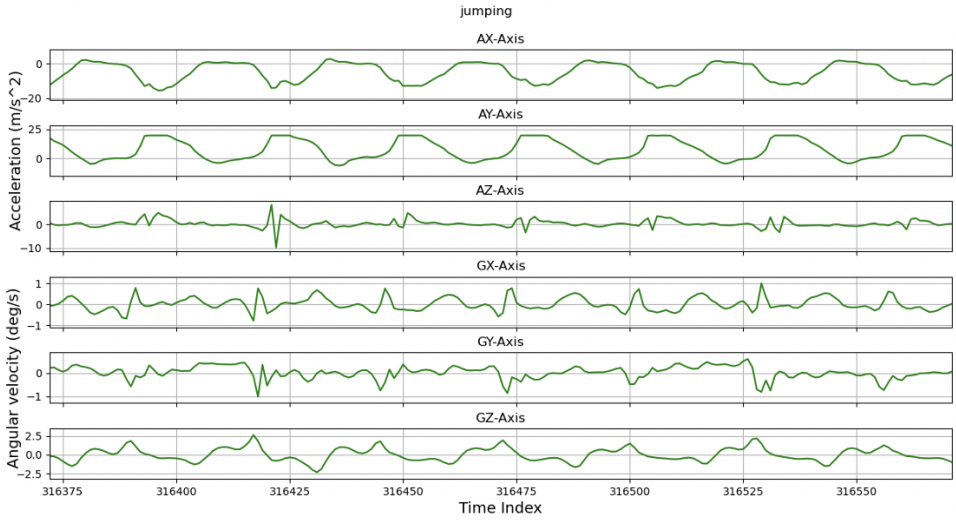

Figure 2.7. Visualization plot of 1-trial data of Jumping activity with six axes belonging to all subjects.

3. SENSOR-WISE PHYSICAL ACTIVITY DETECTION METHOD (SwPAD)

3.1 Data Preprocessing

The raw accelerometer and gyroscope data of Physical Activity Detection sensors from the wearable devices are highly fluctuating over time, increasing the complexity for classification. Therefore, all data used for the study undergo three steps of pre-processing [21] operation: Data Selection, Normalization, Segmentation before training the classifier. Then the data is fed into the deep learning models for PAD.

3.2 Deep learning architecture

The architecture of the SwPAD method consists of several layers such as convolutional layers, max-pooling layers, dropout layer, dense layer, and a training model function to generate precise classification results. The CNN model [22] [23] proposed in this procedure includes four convolutional layers. As shown in Fig. 3.1, the higher layers use broader filters to process more complex input parts. Each convolutional layer describes how CNN captures local dependencies and the scale-invariant characteristics of the activity signals. Each Conv2d layer in the architecture is followed by a leaky rectified linear unit (leaky ReLU) as an active function. The max-pooling layer achieves the scale-invariant feature preservation. In this layer, features from the convolutional layer are split into several partitions. In each partition, we apply a max operation to output the values. Furthermore, same padding is applied in order to save the information of edge from input data of each model.

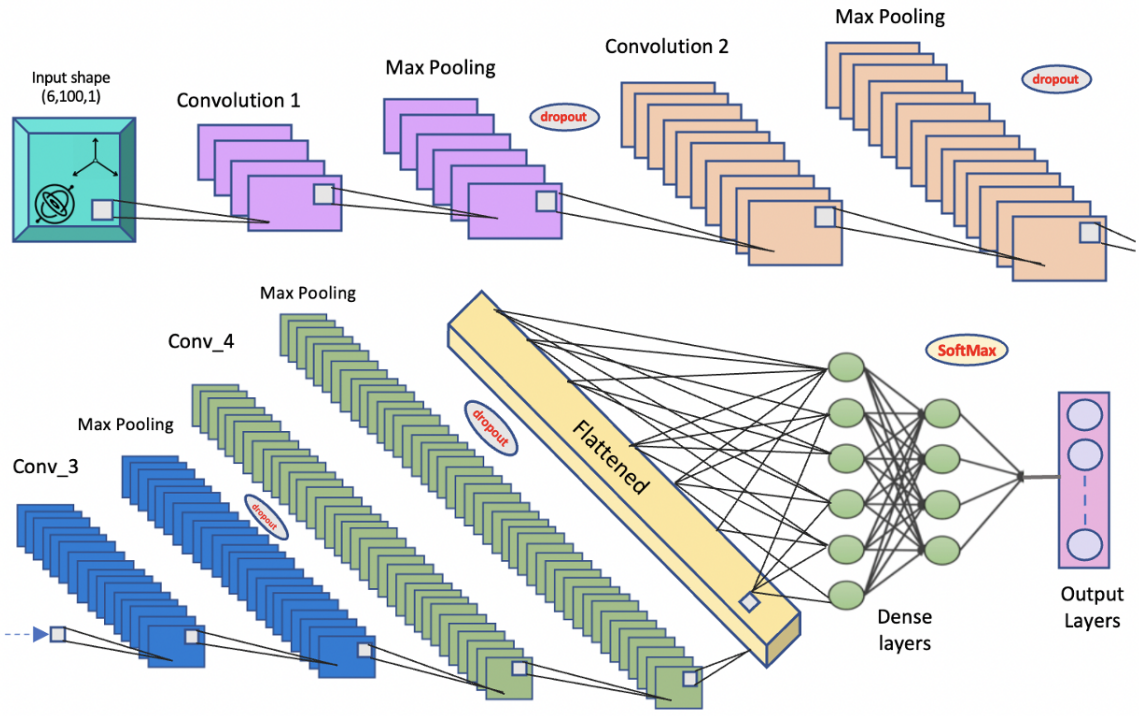

Figure 3.1. Deep learning architecture system for Sensor wise Physical Activity Detection. Evaluation of 2D CNN model with six channel pre-processed input dataset. Seven output models are generated for each sensor location. Notes. Conv-3: Convolution layer 3

Dropout [24] is a simple optimization technique widely used in deep neural network optimization. The units to be dropped are chosen at random. We train a network with dropout by using the approximate averaging method at test time resulting in lower generalization error on different types of classification problems. The parameters used for each layer are mentioned in Table 3.1, the input shape for this method is (6,100,1), and there are seven output models generated, one for each sensor location.

Table 3.1. Different layers of Deep learning architecture and their parameters for training model in Sensor wise Physical Activity Detection method.

Activation	**Layers**	**Parameters**	**Values**
ReLu	Convolution 1	Kernel size	(1,2)
		Filters	16
	Maxpooling		(1,2)
	Dropout		0.15
ReLu	Convolution 2	Kernel size	(1,2)
		Filters	32
	Maxpooling		(1,2)
	Dropout		0.15
ReLu	Convolution 3	Kernel size	(1,2)
		Filters	32
	Maxpooling		(1,2)
	Dropout		0.15
ReLu	Convolution 4	Kernel size	(1,2)
		Filters	64
	Maxpooling		(1,2)
	Dropout		0.15
ReLu	Dense 1		512
	Dropout		0.2
ReLu	Dense 2		256
	Dropout		0.2
Softmax	Dense		num_classes

3.3 Sensor Selection: SxPAD

There are seven sensors used in this study which are placed at the following locations: chest, forearm, head, shin, thigh, upperarm, and waist. There are seven classification models generated in this procedure. They are ranked based on accuracy, and the graph is plotted as shown in Fig. 7.3. The accuracy comparison of these models shows that the highest prediction activity is done by chest and thigh sensors. The forearm and upper arm produced weak accuracy results. It is crucial to choose the best sensor location by considering all factors instead of just going by the highest value. On understanding the practical application, the thigh sensor location is chosen for further study. Holding a device near the thigh region is more feasible than in other locations. It would be more comfortable to slide a device into our pocket instead of holding it in the chest, head, or shin region. Hence, the Thigh sensor location is selected.

3.4 Evaluation methods

We can evaluate the performance of a machine learning algorithm using the train test split method. It can be used for regression, classification problems, and supervised learning algorithms as well. Here, the dataset is divided into two subsets: The training dataset, testing dataset. The former is used to fit the machine learning model, and the latter is used to evaluate based on the results from the previously trained model. Finally, the whole dataset is split into two by 80:20 ratio. We have used the most common split percentage of 80% training set and 20% testing set to obtain satisfactory results.

Training the CNN model with a large dataset is an extensive process due to the time it takes to perform the algorithm. So, we have chosen [25] GPU-based platform to boost the process. We make use of the CUDA platform from NVIDIA. The CNN model is executed using the Keras library.

The PAD model is evaluated based on the results from the classification report consisting of accuracy, recall, precision, and f1-score. We assume that TP, FN, FP, and TN indicate represent the true positive, false negative, false positive, and true negative in binary classification [26]. The formulae for the four evaluation indicators are as follows:

Accuracy = TP+TN/ (TP+FP+FN+TN)

Precision = TP/ (TP+FP)

Recall = TP/ (TP+FN)

F1 Score = 2TP / (2TP+FP +FN)

The sci-kit learn library is imported to perform this computation. The results are visually represented using a ranking plot. Each model was executed twice with a different random seed value at each iteration. The average of both these models was considered for final evaluation. The desired results were obtained by following this method.

4. SENSOR AND CHANNEL WISE PHYSICAL ACTIVITY DETECTION METHOD (SCwPAD)

4.1 Deep learning architecture

The architecture of the SCwPAD method also consists of convolutional layers, max-pooling layers, dropout layer, dense layer, and a training model function. The CNN model [4] proposed in this includes three convolutional layers. The overall set up is similar to the one implemented in Chapter 3 and processes data at each layer as shown in Fig 4.1. The parameters used for each layer are mentioned in Table 4.1. The input shape is (1,100,1) as only one channel is considered for a single model. A fixed random seed value is defined during model evaluation, and therefore at each iteration, the same transformation is executed. There are 42 output models generated.

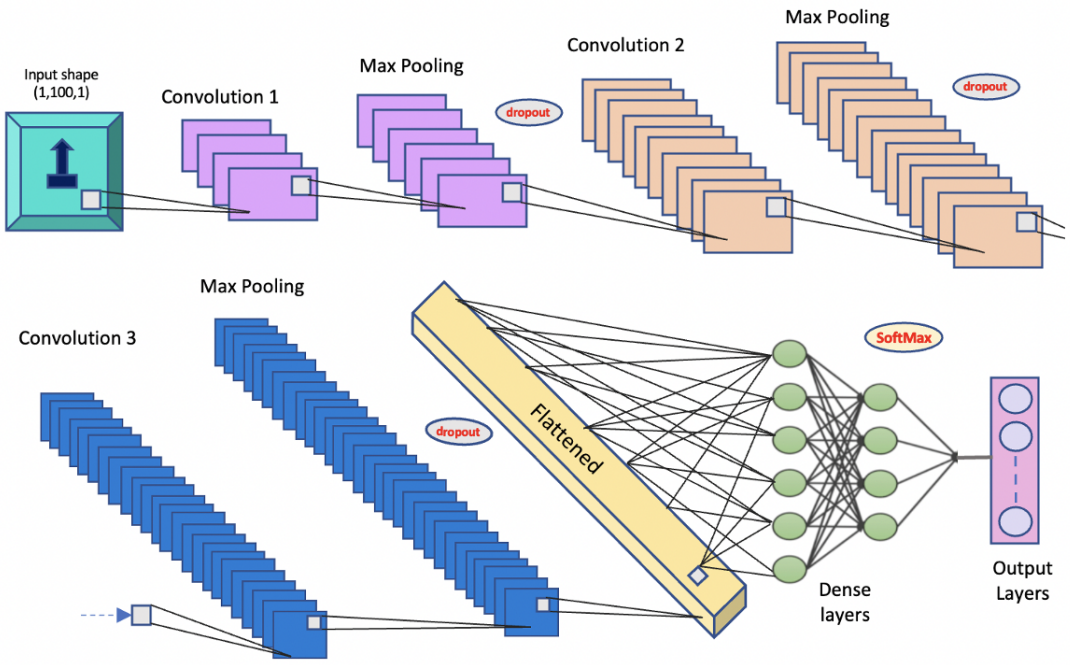

Figure 4.1. Deep learning architecture system for Sensor and Channel wise Physical Activity Detection. Evaluation of 2D CNN model with a single channel pre-processed input dataset. Forty-two output models are generated for each possible combination of sensor location and channel type.

Table 4.1. Different layers of Deep learning architecture and their parameters for training model in Sensor and Channel wise Physical Activity Detection method.

Activation	Layers	Parameters	Values
ReLu	Convolution 1	Kernel size	(1,2)
		Filters	16
	Maxpooling		(1,2)
	Dropout		0.15
ReLu	Convolution 2	Kernel size	(1,2)
		Filters	32
	Maxpooling		(1,2)
	Dropout		0.15
ReLu	Convolution 3	Kernel size	(1,2)
		Filters	32
	Maxpooling		(1,2)
	Dropout		0.15
ReLU	Dense 1		512
	Dropout		0.2
ReLU	Dense 2		256
	Dropout		0.2
Softmax	Dense		num_classes

4.2 Sensor Selection: SCxPAD

The comparison of accuracy ranking of the model showed that the values from channels belonging to Shin and Thigh sensor give the best prediction. The accelerometer - y channel yielded the highest accuracy percentage. A single channel from a sensor must be selected from the 42 models present for further study compared to Sensor Channel selection. Therefore, from careful analysis and data from the previous method, the accelerometer y-channel from the thigh sensor is selected for further study.

4.3 Evaluation methods

The evaluation of the model classified based on SCwPAD method is done using comparison of performance metrics [27] such as accuracy, precision, recall and F1-score as performed in the previous method in Chapter 4.

5. TRANSFER LEARNING FOR SxPAD

5.1 Direct learning strategy

In the Direct learning strategy, the method directly involves the analysis of the target dataset. They provide accurate prediction results, as the input does not involve data from other sources. The selected thigh sensor from each of the 15 subjects forms the input dataset. The dataset is focused only on the selected sensor from analysis performed previously in Chapter 3. The dataset corresponding to thigh sensor location from each subject is used for the study.

5.2 Transfer learning Methodology

The procedure involves training a particular model using information from other sources that do not involve the subject under study. It attempts to exhibit that data from previously trained models can be re-used to perform a new analysis. We transfer a part of already trained layers and combine them with few new layers to train data in the new task. The block diagram of transfer learning model [28] [29] for SxPAD is shown in Fig. 5.1. Our project is suitable for this method as we possess enough labeled data for training. The dataset is focused only on the selected sensor from analysis performed previously in Chapter 3. The dataset corresponding to thigh sensor location from each subject is used for the study.

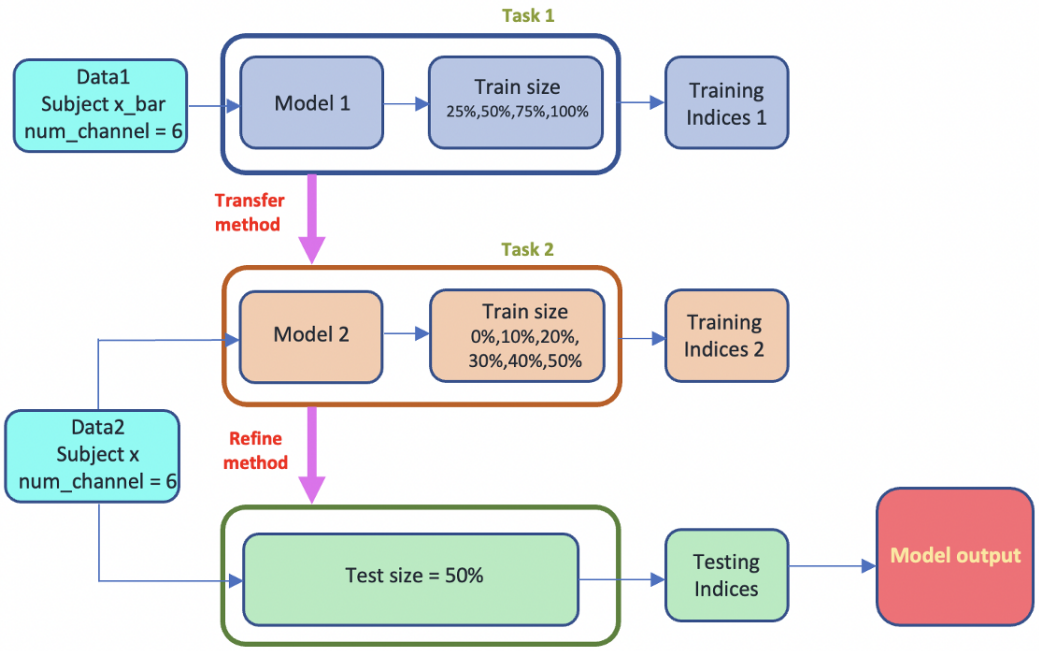

Figure 5.1. Block diagram of Transfer learning architecture for Sensor - x - Physical Activity Detection. The training indices are generated from sources other than the subject under study. Evaluation of 2D CNN model is trained using both transfer and refine the method. Input is a six-channel pre-processed dataset consisting of data corresponding to the selected Sensor location. Notes. Subject x: dataset belonging to that subject, Subject x-bar: dataset generated by combining information of all other subjects except subject x.

6. TRANSFER LEARNING FOR SCxPAD

6.1 Direct learning strategy

The Direct learning strategy is a method that directly involves the analysis of the target dataset. Accurate prediction results are generated since data from other sources are not included in the input. The dataset is focused only on the selected sensor location and sensor channel type from analysis performed previously in Chapter 3 and Chapter 4. The accelerometer-y channel corresponding to thigh sensor location is the dataset under study.

6.2 Transfer learning Methodology

In this method, we use data from other sources as input to the target model. We classify the model in the new task using pre-trained layers and combine them with few new layers. The block diagram of transfer learning [28] [29] model for SCxPAD is shown in Fig. 6.1. The dataset is focused only on the selected sensor location and sensor channel type from analysis performed previously in Chapter 3 and Chapter 4. The accelerometer-y channel corresponding to thigh sensor location from each subject is the dataset under study.

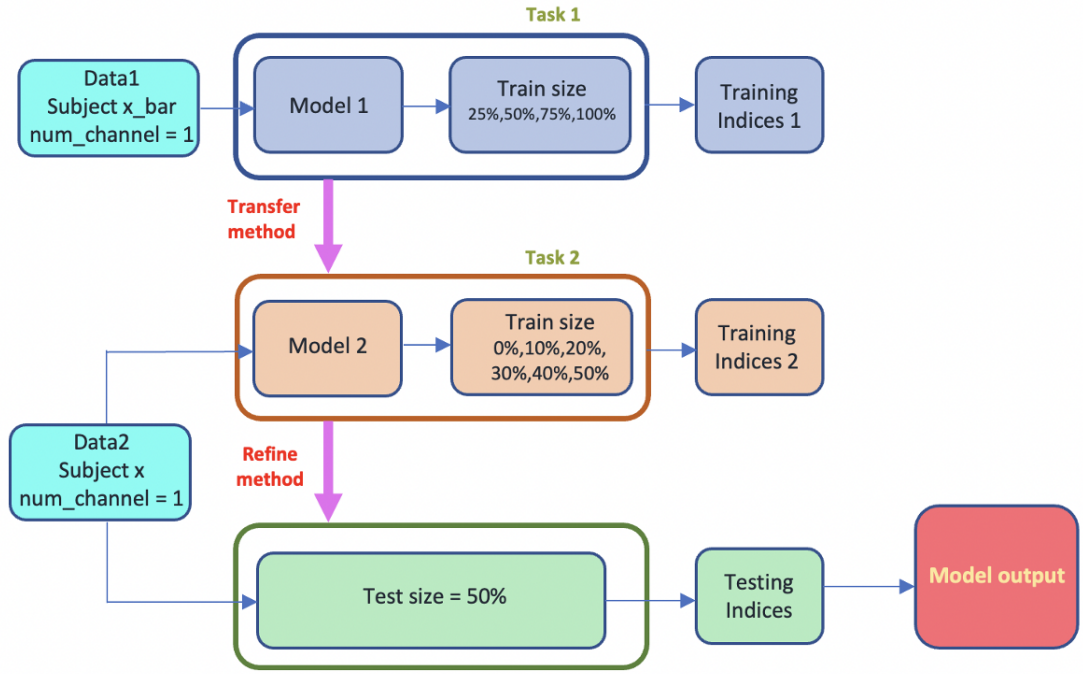

Figure 6.1. Block diagram of Transfer learning architecture for Sensor and Channel - x - Physical Activity Detection. The training indices are generated from sources other than the subject under study. Evaluation of 2D CNN model is trained using both transfer and refine the method. Input is a single-channel pre-processed dataset consisting of data corresponding to the selected Sensor location and channel type. Notes. Subject x: dataset belonging to that particular subject, Subject x-bar: dataset generated by combining information of all other subjects except subject x.

7. RESULTS

7.1 Experimental Setup

The Real-world dataset [17] chosen for our study outwits all these complaints as the data was generated from 15 subjects (8 males, seven females) donning seven smart wearable devices on their bodies at different positions [30]. They traveled in all kinds of demographic areas such as Downtown, suburbs, forests, and parks. The tri-axial accelerometer and gyroscope values are selected for this study. Climbing up, climbing down, walking, running, lying, and jumping are the six activities performed by the 15 subjects for approximately 10 minutes (except jumping – 2 minutes)

7.2 SwPAD

The learning curve is a visual representation of the training model [31]. The slope of the learning curve indicates the rate at which the accuracy and loss improve as a model is trained using a deep learning algorithm. Fig. 7.1 represents seven deep learning curves generated by training models based on seven different sensor locations.

The confusion matrix is used to evaluate the quality of output of a classifier on the PAD dataset. The total number of points for which the predicted label is equal to the true label is represented by the elements in the diagonal of the matrix, while those that don't belong to the main diagonal are elements that are mislabeled by the classifier [32]. Fig. 7.2 shows seven confusion matrices generated from the classifying model based on SwPAD. The correct predictions are identified by the number of diagonal values present in the confusion matrix, which indicates many correct predictions. The classification model is based on the type of activity.

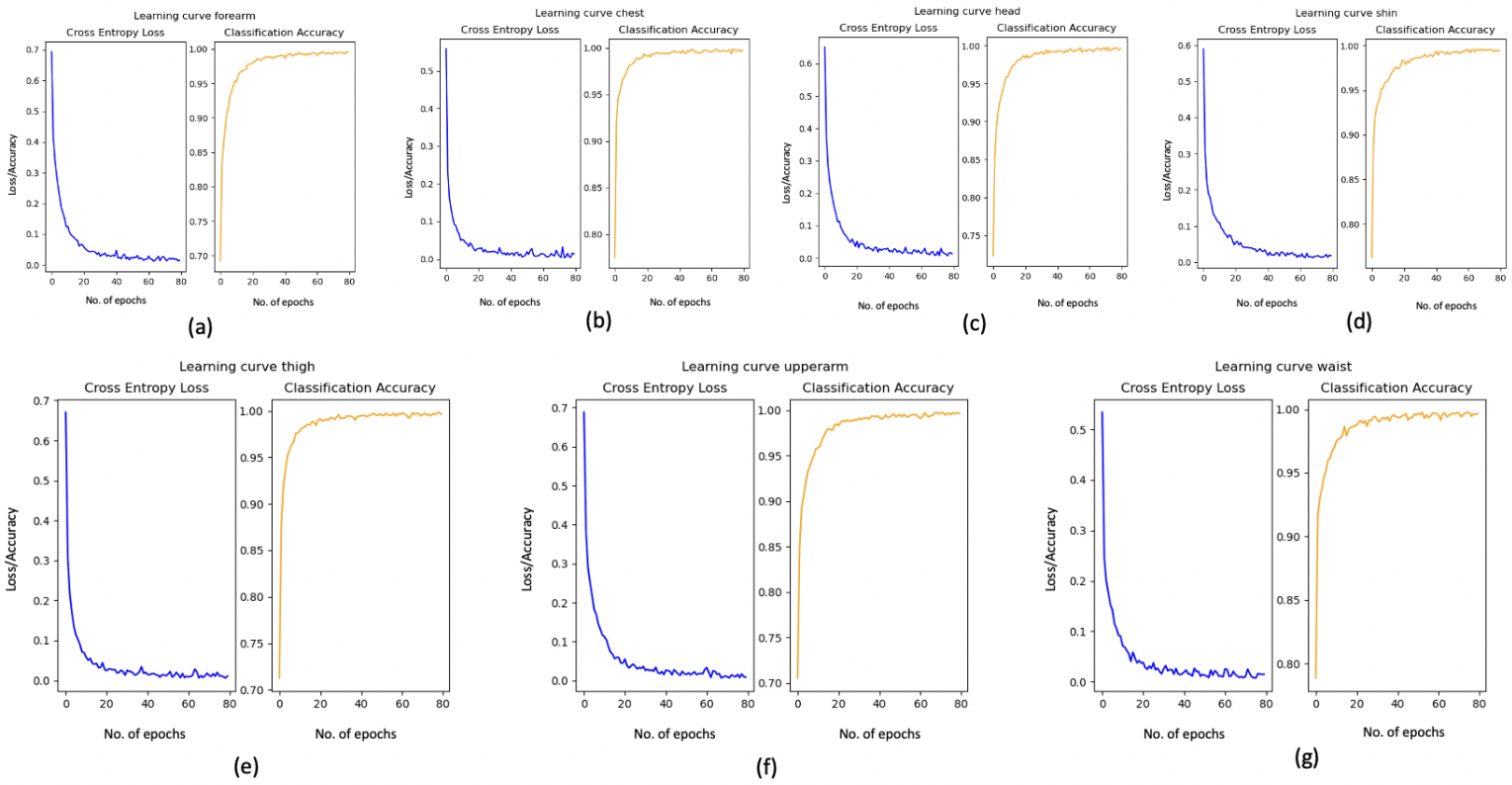

Figure 7.1. Seven Deep learning curves of loss and accuracy for each sensor location generated while training the model in SwPAD method. (a). Forearm sensor, (b). Chest sensor, (c). Head sensor, (d). Shin sensor, (e). Thigh sensor, (f) Upperarm sensor, and (g). Waist sensor. Notes. num-epochs =80.

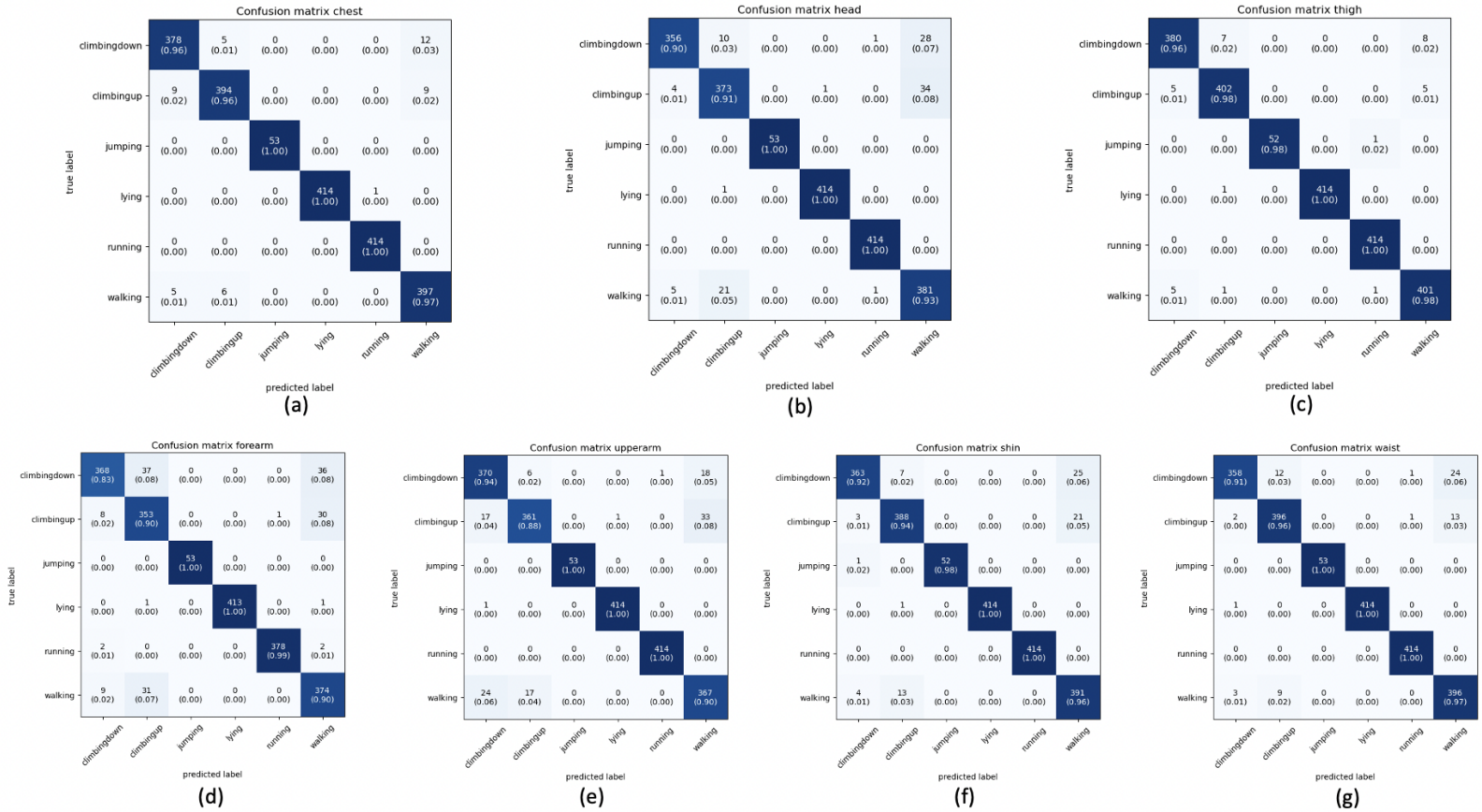

Figure 7.2. Seven confusion matrices for each sensor location depicting the classification of CNN models in the SwPAD method. (a). Chest sensor, (b). Head sensor, (c). Thigh sensor, (d). Forearm sensor, (e). Upperarm sensor, (f) Shin sensor and (g). Waist sensor. Notes. num-classes = 6

The classification accuracy is the total number of correct predictions divided by the total number of predictions made for a dataset. The accuracy results from the SwPAD model generated for each sensor location are visualized as a ranking plot to analyze the prediction trend of each sensor, as shown in Fig. 7.3. The highest accuracy value was generated by thigh sensor location.

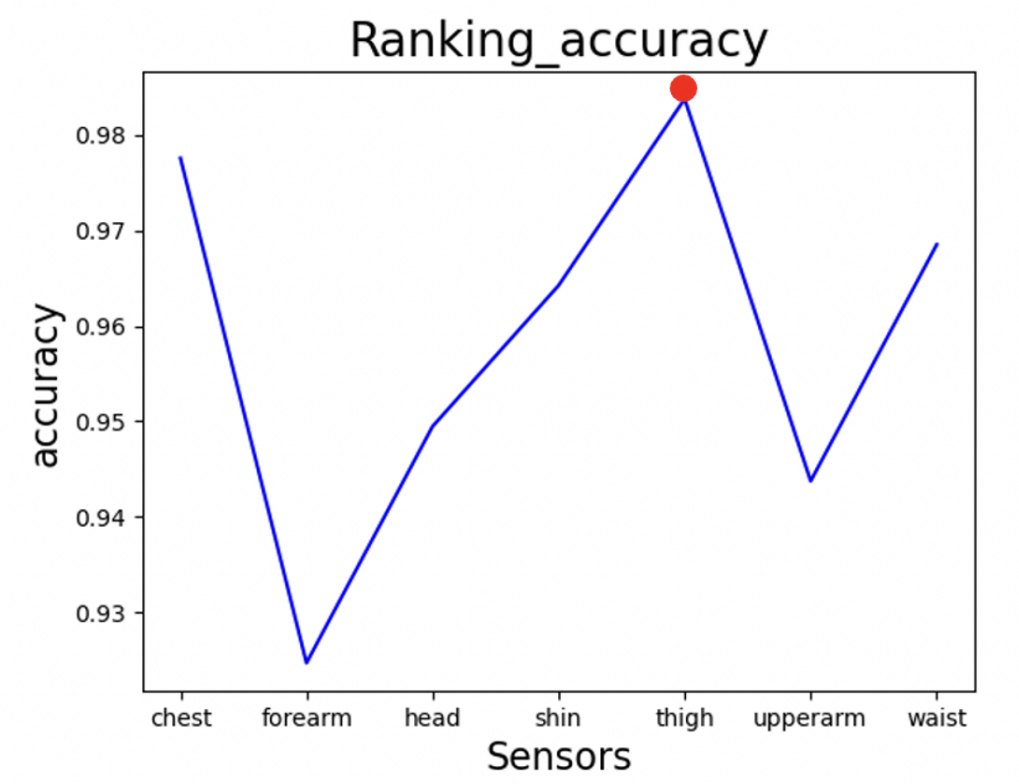

Figure 7.3. Accuracy ranking plot generated from the performance analysis of all seven sensor locations in SwPAD method. The highest accuracy is obtained at the thigh sensor location.

The terms precision, recall, and f1-score relate to getting a finer-grained idea of how well a classifier is doing instead of just looking at overall accuracy. Precision is a measure of how many of the positive predictions made are correct. [33] The recall measures how many of the positive cases the classifier correctly predicted, i.e., overall positive cases in the data. It is sometimes also referred to as Sensitivity. F1-Score combines both precision and recall and is generally described as the harmonic mean of the two. The visualization of precision, recall, and F1-measure is shown in Fig. 7.4, Fig. 7.5, and Fig. 7.6, respectively.

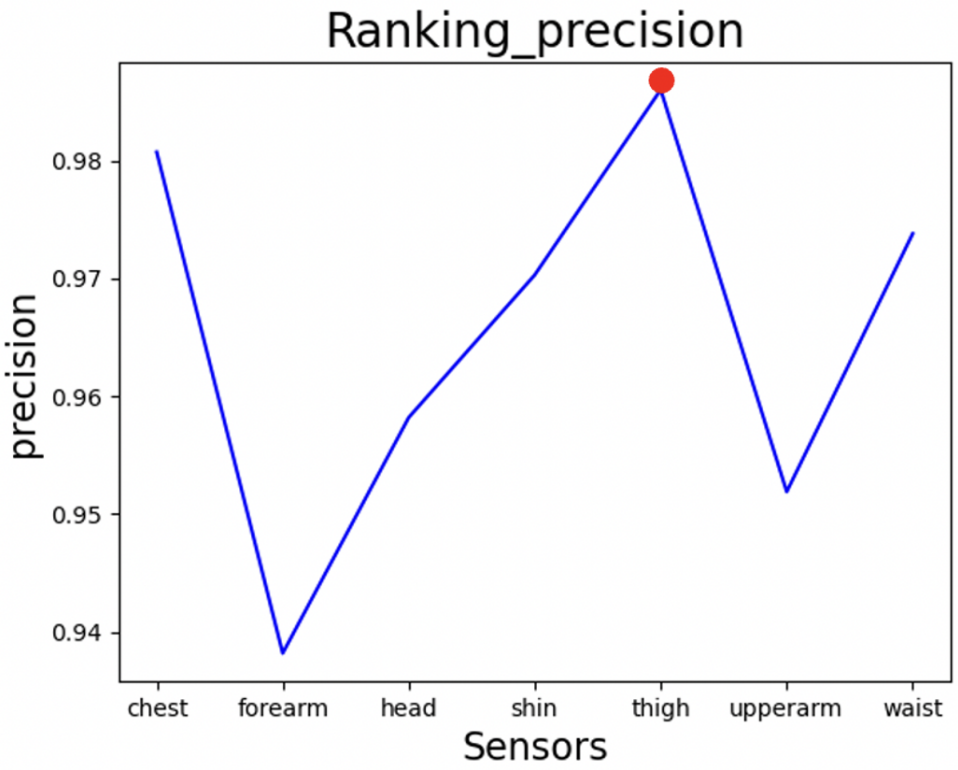

Figure 7.4. The precision ranking plot from the performance analysis of all seven sensor locations in the SwPAD method. The highest precision is obtained at the thigh sensor location.

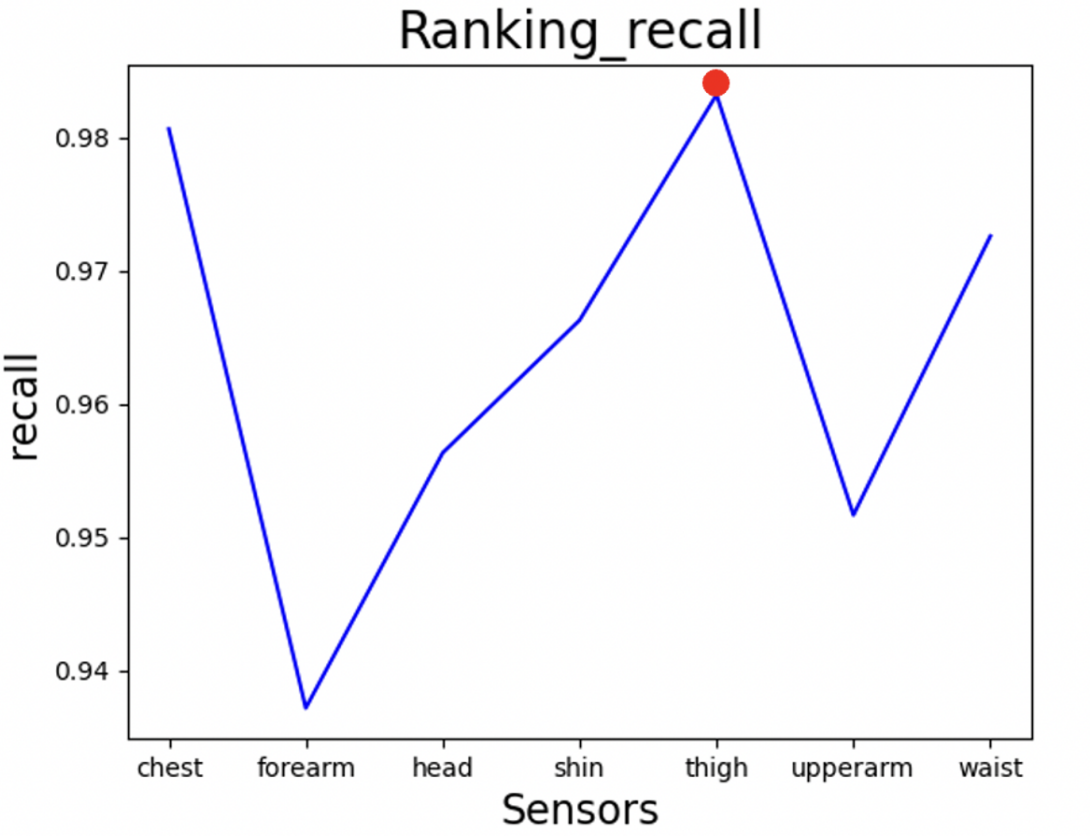

Figure 7.5. The ranking plot of recall parameter from the performance analysis of all seven sensor locations in the SwPAD method. The maximum recall value is obtained at the thigh sensor location.

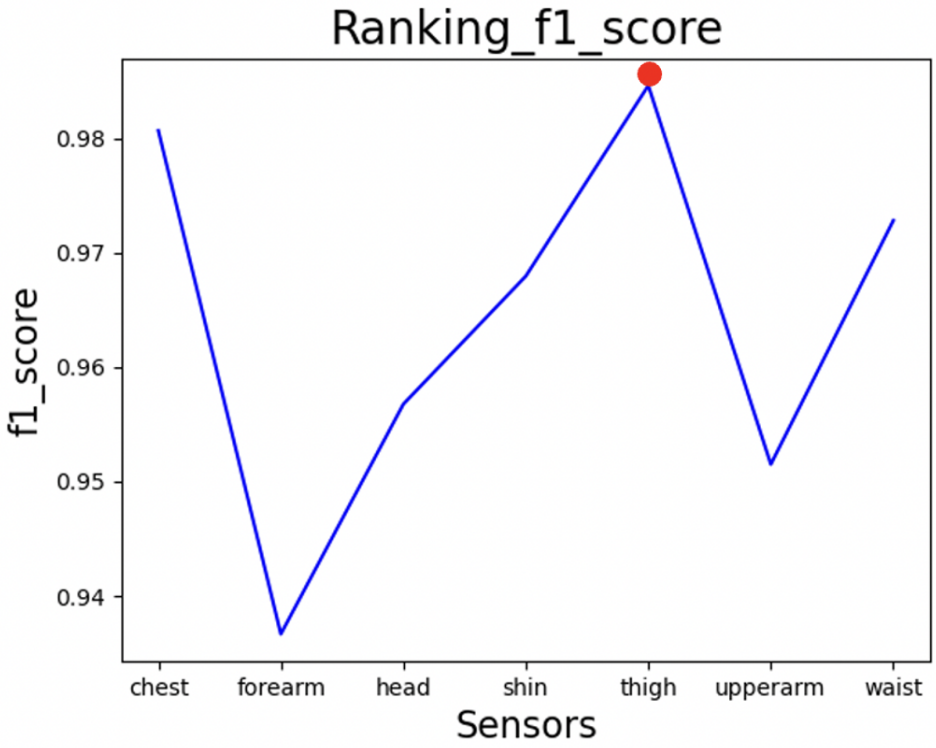

Figure 7.6. Ranking plot of F1-measure from the performance analysis of all seven sensor locations in SwPAD method. The maximum F1-score is obtained at the thigh sensor location.

7.3 SCwPAD

Seven selected deep learning curves generated by the training model based on six channel types and seven sensor locations are shown in Fig. 7.7. The diagonal elements from the confusion matrices are studied to determine which combination generated the best classification model, as shown in Fig. 7.8. A total of forty-two models are analyzed, and the best sensor and channel type is chosen for the analysis in SCxPAD.

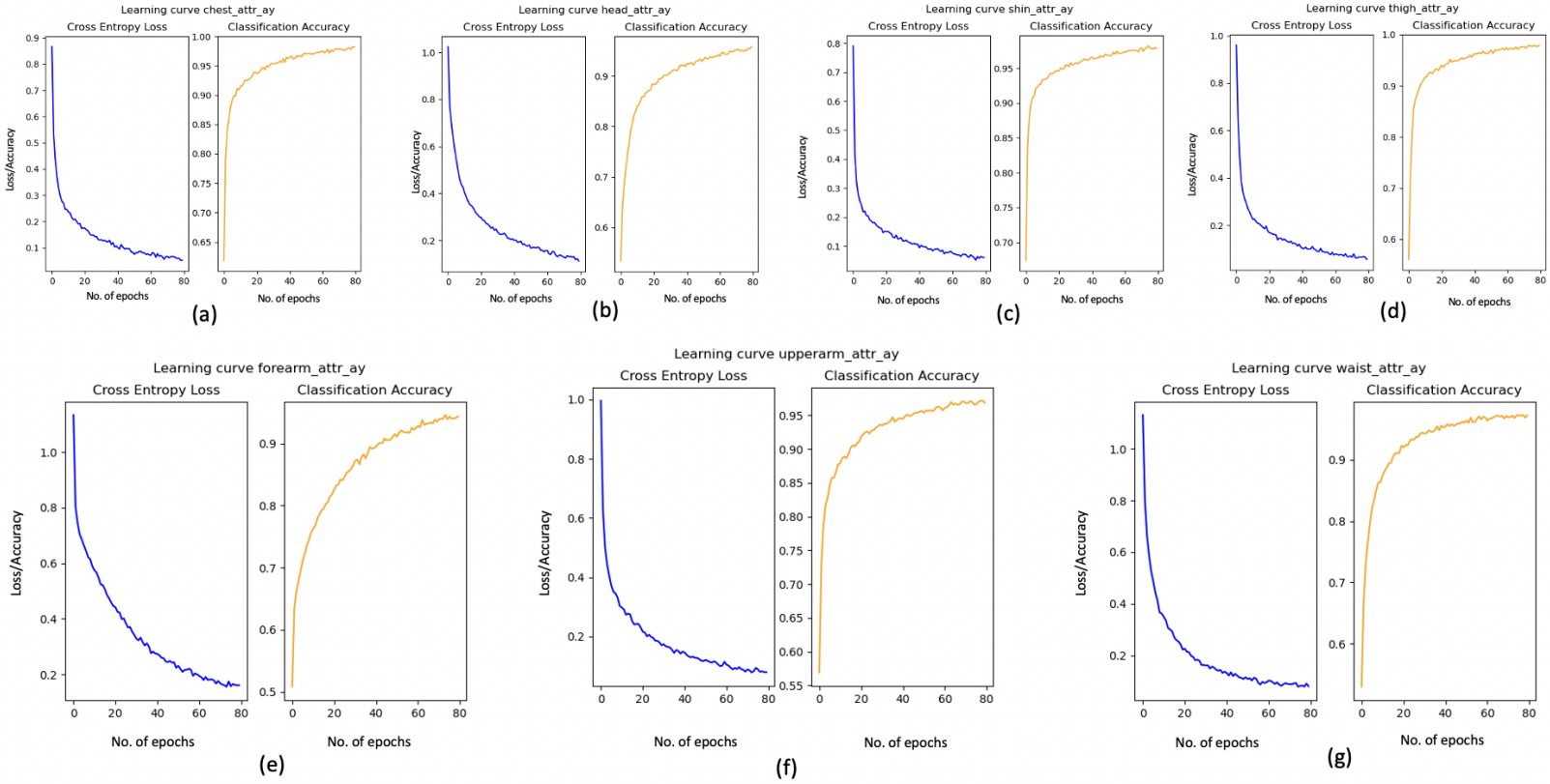

Figure 7.7. The Deep learning curve of loss and accuracy for a selected channel type of each sensor location is generated while training the model in the SCwPAD method. (a). Forearm sensor, (b). Chest sensor, (c). Head sensor, (d). Shin sensor, (e). Thigh sensor, (f) Upperarm sensor, and (g). Waist sensor. Notes. num-epochs =80, selected channel = attr-y (accelerometer- y channel)

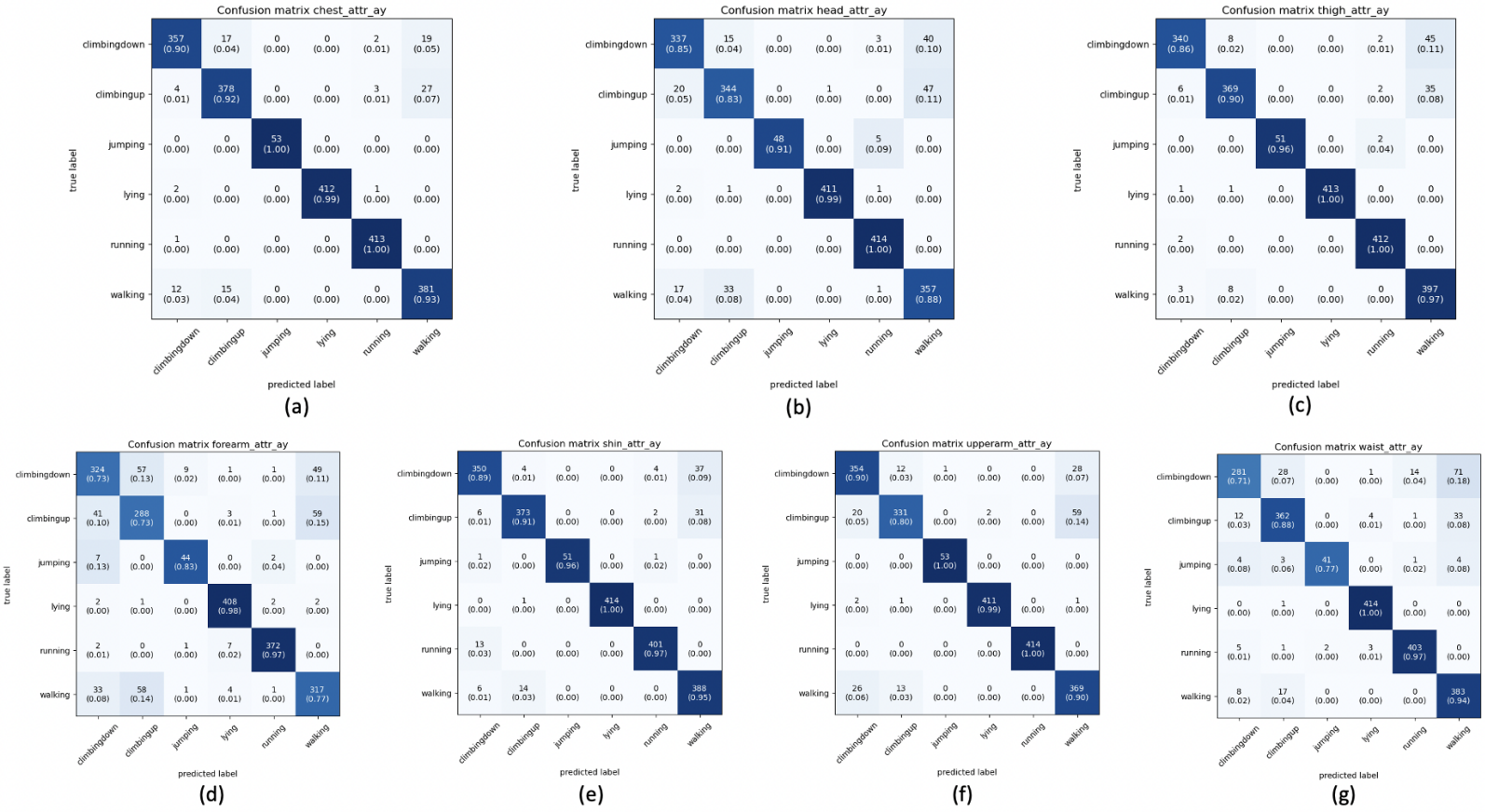

Figure 7.8. Confusion matrices of a selected channel type for each sensor location depicting classification of CNN model in SCwPAD method. (a). Chest sensor, (b). Head sensor, (c). Thigh sensor, (d). Forearm sensor, (e). Upperarm sensor, (f) Shin sensor and (g). Waist sensor. Notes. num-classes = 6, selected channel = attr-ay (accelerometer- y channel)

The visualization of ranking of accuracy, precision, recall, and f1-measure are shown in Fig. 7.9, Fig. 7.10, Fig. 7.11, and Fig. 7.12, respectively. The accelerometer-y channel of the thigh sensor produced the best results and is selected for further study.

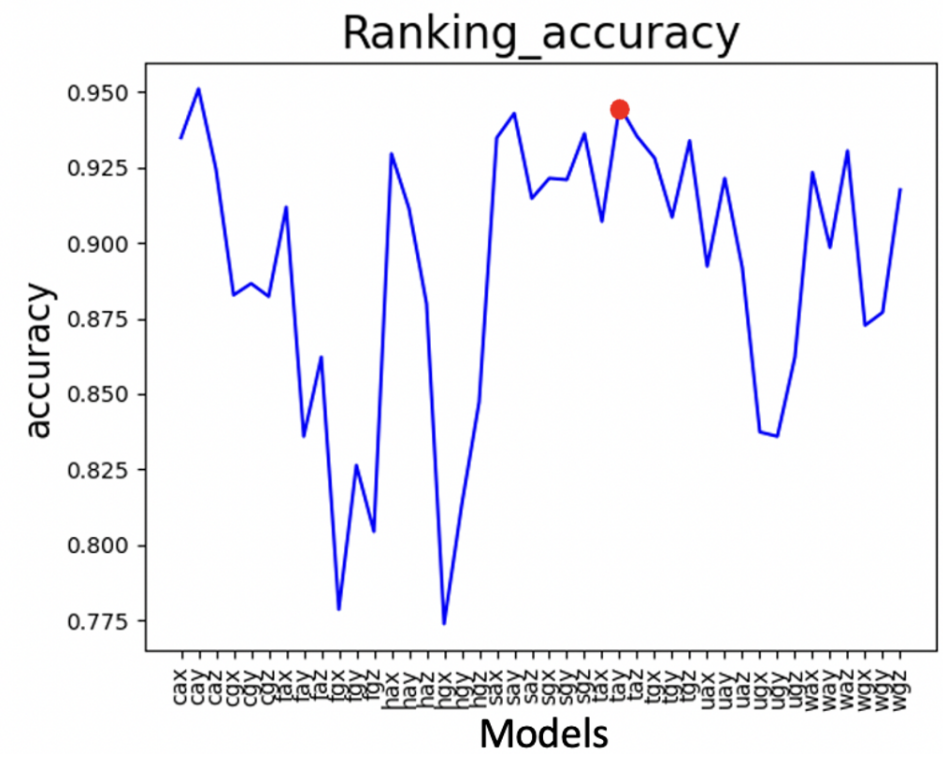

Figure 7.9. Accuracy ranking plot from the performance analysis of all forty-two models in SCwPAD method.

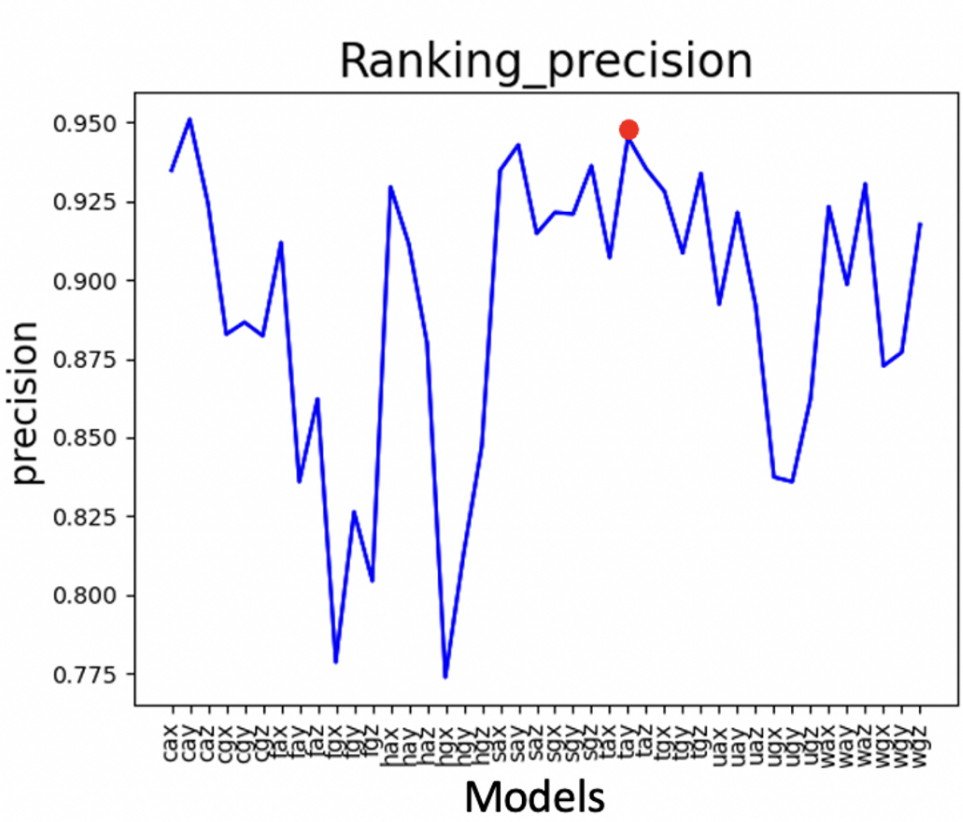

Figure 7.10. The Precision ranking plot from the performance analysis of all forty-two models in the SCwPAD method.

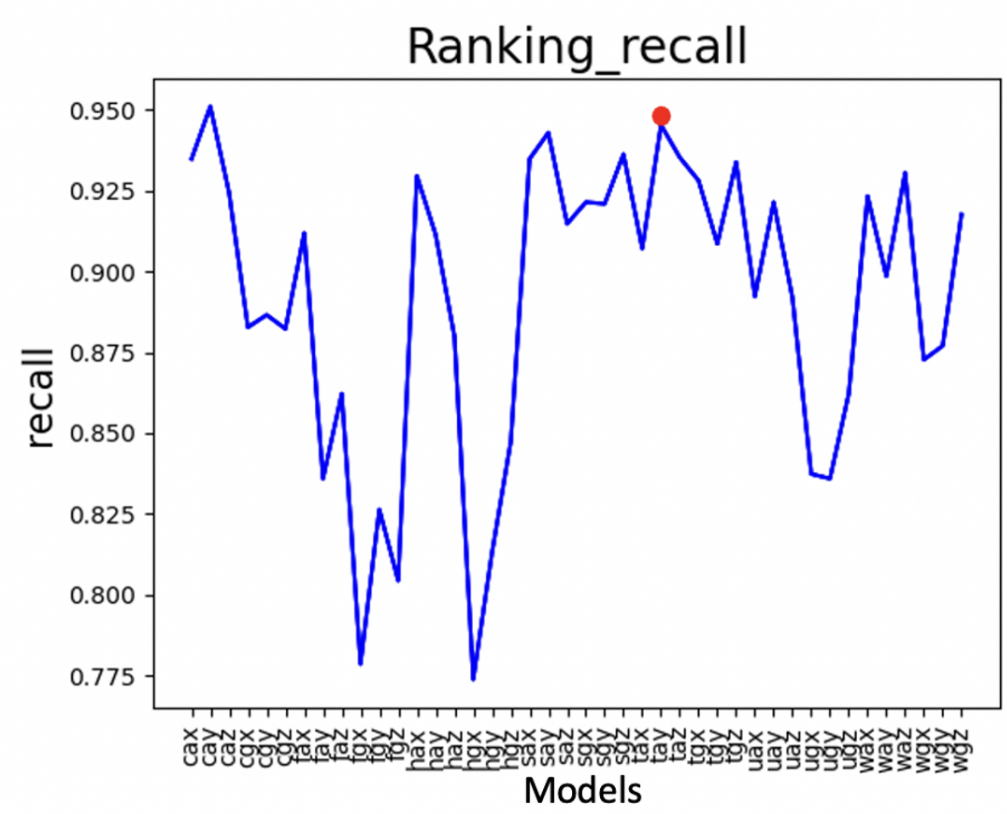

Figure 7.11. The Ranking plot of recall parameter from the performance analysis of all forty-two models in the SCwPAD method.

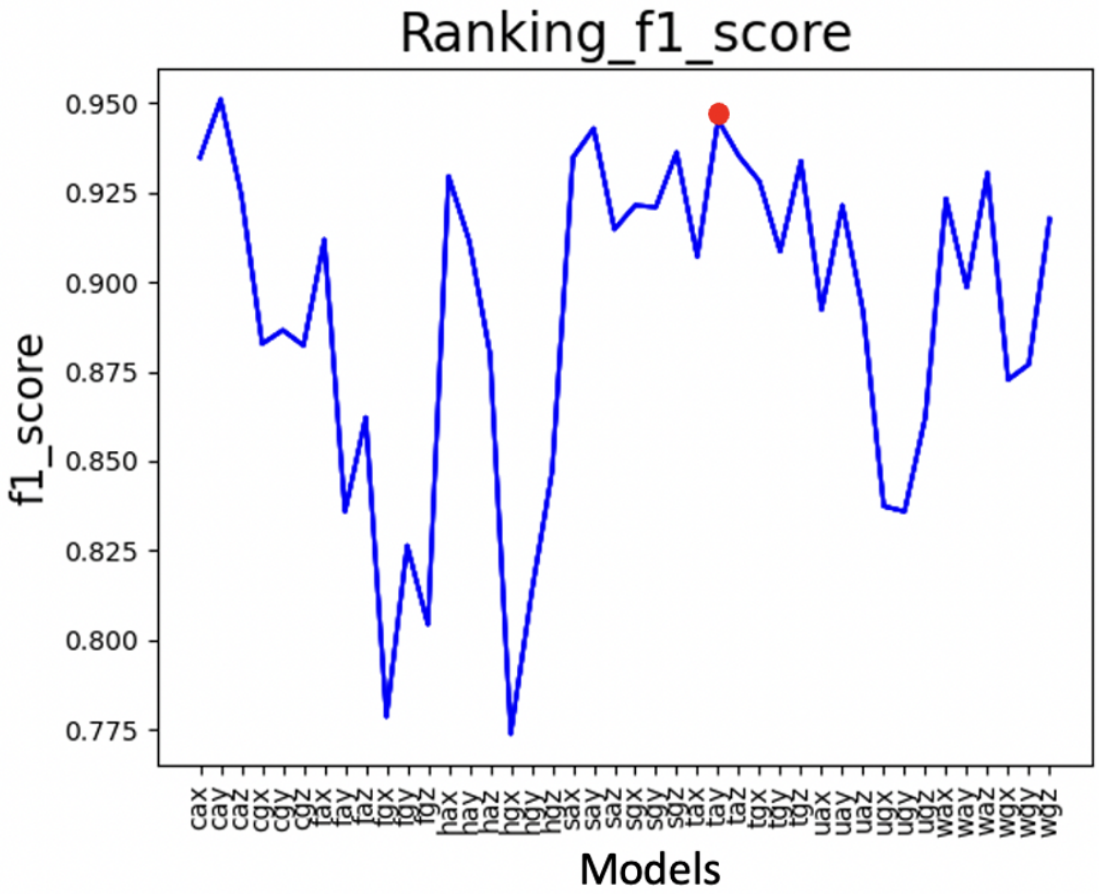

Figure 7.12. The Ranking plot of F1-measure from the performance analysis of all forty-two models in the SCwPAD method.

7.4 Comparison of SwPAD and SCwPAD, and Selection

The results from SwPAD and SCwPAD helps in deciding the optimal sensor and channel type to select for further analysis. By training a model with a specific feature, we obtain a wide range of results and thus can easily choose the model with high efficacy. Hence, feature selection is essential in data analysis for better results in a short duration. By doing so, we reduce the need for computation using large datasets.

7.5 Direct and Transfer Learning for SxPAD

The data from the thigh sensor location is being analyzed in this method. In direct learning, only the subject under study is being trained. In the transfer learning method of SxPAD, the data from thigh sensor location is being. The model is trained twice. The refine method, where the only subject under study is used, and two, the transfer method, wherein data from all other sources are used. The test dataset is the same throughout the study.

In direct learning, the model selected is thigh sensor location. It can be viewed that accuracy increases with an increase in training size. Fig. 7.13 shows the accuracy ranking averaged across all the subjects. The training percentage of subject x is 10%, 20%, 30%, 40%, 50%.

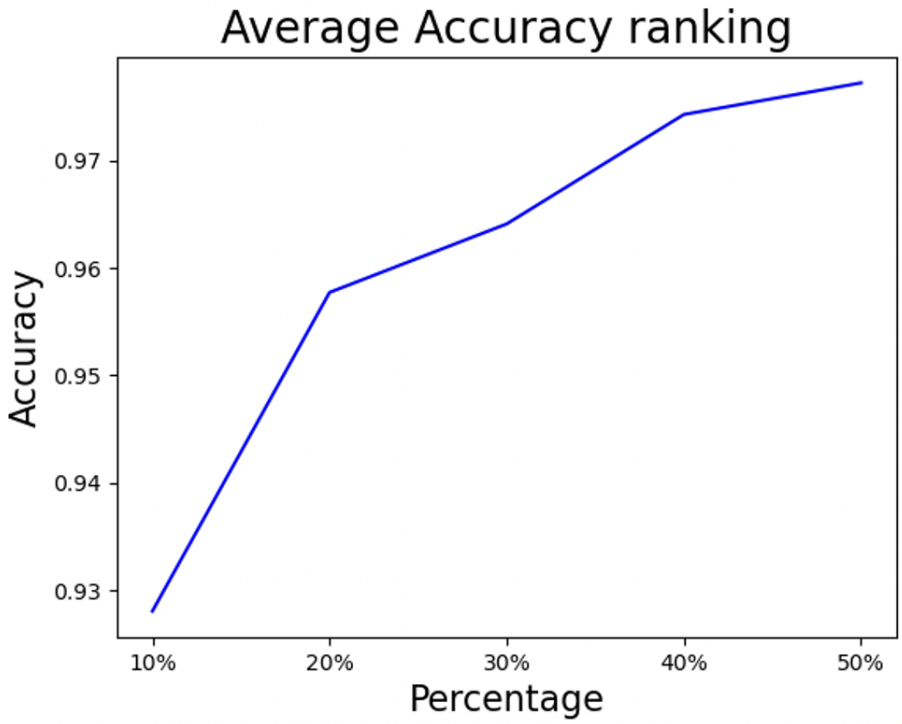

Figure 7.13. Average Accuracy ranking plot from analysis through Direct learning strategy in SxPAD method for different training percentages. The model selected is thigh sensor location.

In transfer learning, the model selected is thigh sensor location. The accuracy curve from direct learning is also projected to observe the trend. The figures show that transfer learning yields better results at training percentage in the initial stages. Fig. 7.14 shows the accuracy ranking averaged across all the subjects.The training percentage of subject x is 0%, 10%, 20%, 30%, 40%, 50% and the training percentage of all other subjects is 25%, 50%, 75%, 100%.

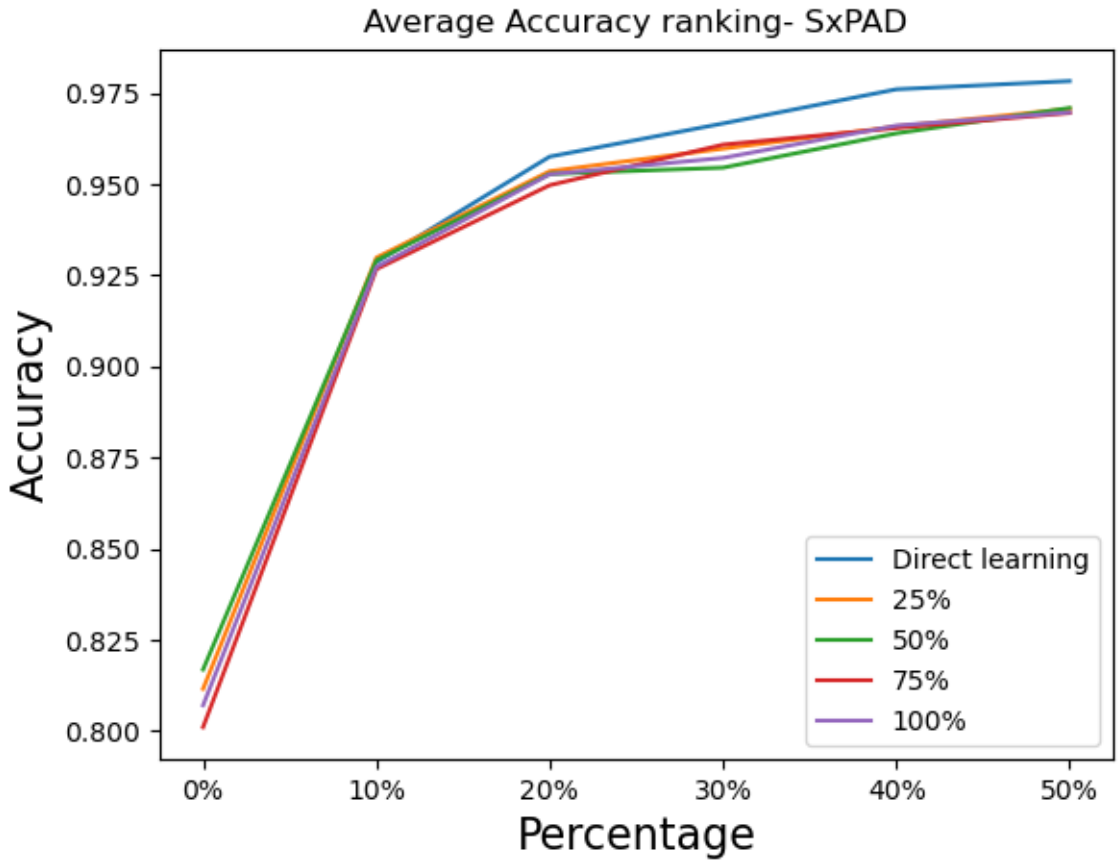

Figure 7.14. The SxPAD average accuracy ranking plot generated by average of two transfer learning simulation implemented with different random seed.

7.6 Direct and Transfer Learning for SCxPAD

The data from the thigh sensor and the accelerometer-y channel is being analyzed in this method. In direct learning, only the subject under study is being trained. In the transfer learning method of SxPAD, the data from thigh sensor location is being. Thus, the model is trained twice. The subject under study is used, called the refine method, and two, data from all other sources, called the transfer method. The test dataset is the same throughout the study.

In direct learning, the model selected is the accelerometer-y channel of thigh sensor location. It can be viewed that accuracy increases with an increase in training size. Fig. 7.15 shows the accuracy ranking averaged across all the subjects.The training percentage of subject x is 10%, 20%, 30%, 40%, 50%.

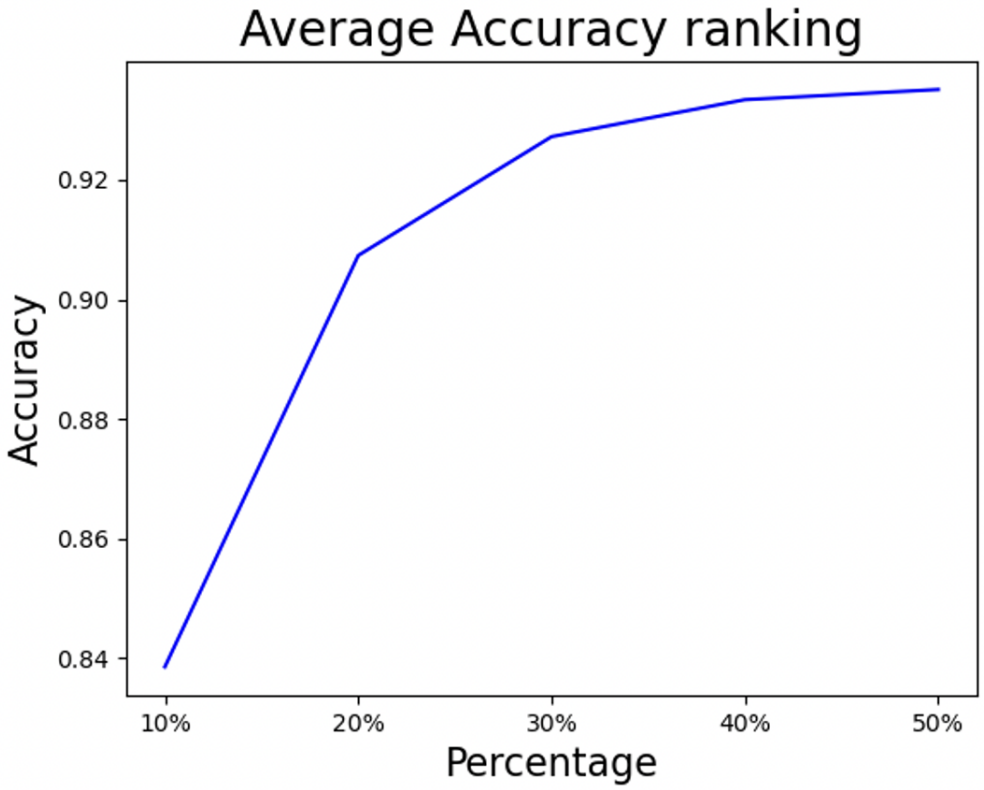

Figure 7.15. Average Accuracy ranking plot from analysis through Direct learning strategy in SCxPAD method for different training percentages.

In transfer learning, the model selected is the accelerometer-y channel of thigh sensor location. The accuracy curve from direct learning is also projected to observe the trend. The figures show that transfer learning yields better results at training percentage in the initial stages. The accuracy ranking averaged across all the subjects is shown in Fig 7.16.The training percentage of subject x is 0%, 10%, 20%, 30%, 40%, 50% and the training percentage of all other subjects is 25%, 50%, 75%, 100%.

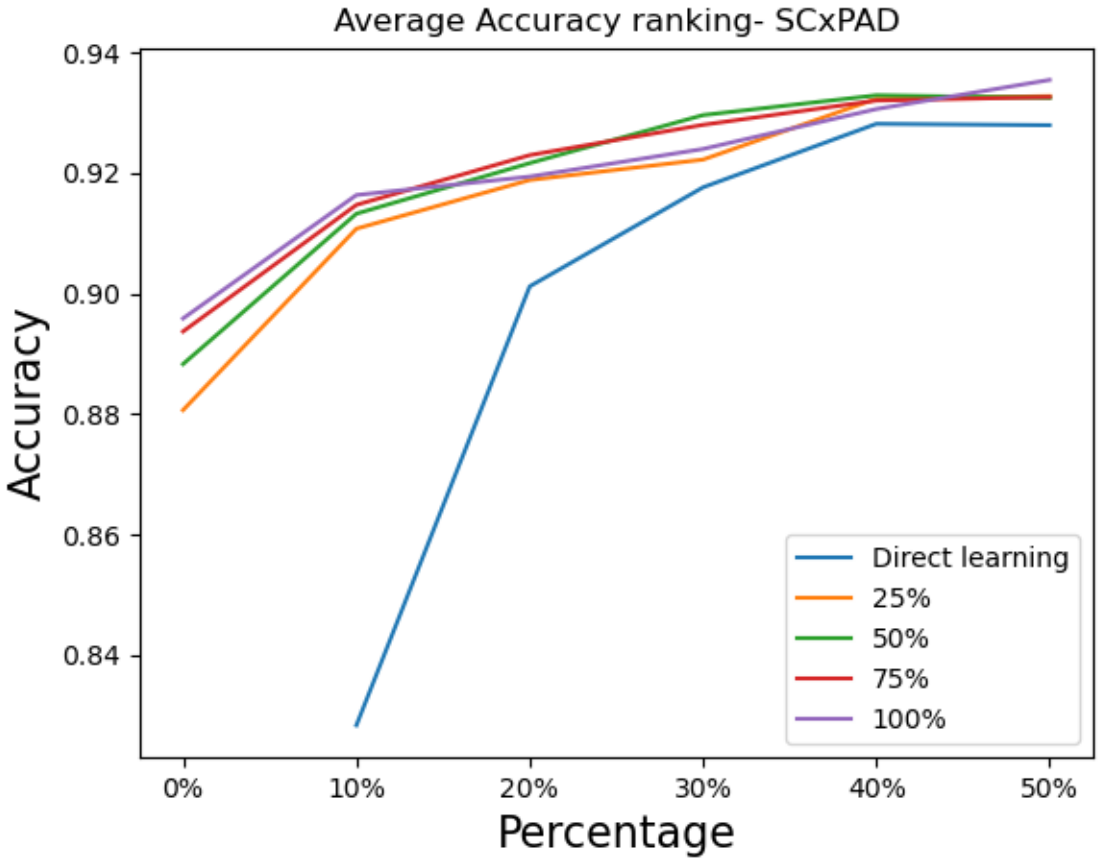

Figure 7.16. The SCxPAD average accuracy ranking plot generated by average of two transfer learning simulation implemented with different random seed.

7.7 Comparison of Transfer Learning for SxPAD and SCxPAD

The results from SxPAD and SCxPAD demonstrates the effectiveness of transfer learning [34]. By training the model using pre-trained results that can give better prediction results than the traditional method, we save much time in computing the complex deep learning algorithm repeatedly. By comparing the average accuracy ranking from Fig. 7.14 and Fig. 7.16, we can understand the advantage of training the model with a single channel type.

8. CONCLUSION

In this project, we have compared and analyzed the biomechanical big data based on location difference of sensor devices using deep learning algorithms. We further compared the six sensor channels [35] (3-axis accelerometer and 3-axis gyroscope). The optimal sensor and channel were selected from the PAD performance model. Furthermore, the proposed transfer learning methodology has been proved effective in minimizing the training effort of the deep learning model. The best prediction was observed for the single channel case. Thus, the research demonstrates potential ultra-low-power PAD with minimized sensor stream and training effort. The experimental evaluation shows the efficiency of this method and validates the proposed wearable device. In conclusion, we have developed an ultra-low-power PAD device to track the health and safety of an individual.

9. FUTURE STUDIES

Future studies may be performed further to enhance the performance of the deep learning models. Furthermore, it is interesting to minimize the training effort additionally during the transfer learning process. Besides, the implementation of PAD in different applications is also fascinating and may advance the field a lot.

REFERENCES

[1] D. Morris, B. Schazmann, Y. Wu, C. Fay, S. Beirne, C. Slater, K. T. Lau, G. Wallace, and D. Diamond, "Wearable technology for the real-time analysis of sweat during exercise," in *2008 First International Symposium on Applied Sciences on Biomedical and Communication Technologies*, 2008, pp. 1–2. DOI: 10.1109/ISABEL.2008.4712603.

[2] X. Niu, Z. Wang, and Z. Pan, "Extreme learning machine-based deep model for human activity recognition with wearable sensors," *Computing in Science Engineering*, vol. 21, no. 5, pp. 16–25, 2019. DOI: 10.1109/MCSE.2018.110145933.

[3] S. Tang, S. Aoyagi, Y. Ho, E. Sato-Shimokawara, and T. Yamaguchi, "Wearable sensor data visualization based on cnn towards healthcare promotion," in *2020 International Symposium on Community-centric Systems (CcS)*, 2020, pp. 1–5. DOI: 10.1109/CcS49175.2020.9231517.

[4] Y.-J. Lin, C.-W. Chuang, C.-Y. Yen, S.-H. Huang, P.-W. Huang, J.-Y. Chen, and S.-Y. Lee, "Artificial intelligence of things wearable system for cardiac disease detection," in *2019 IEEE International Conference on Artificial Intelligence Circuits and Systems (AICAS)*, 2019, pp. 67–70. DOI: 10.1109/AICAS.2019.8771630.

[5] J. Castañó, "10 machine learning methods that every data scientist should know," *Towards Datascience*, May, 2019, Last accessed: 10/07/2021. [Online]. Available: https://towardsdatascience.com/10-machine-learning-methods-that-every-data-scientist-should-know-3cc96e0eeee9.

[6] M. Batool, A. Jalal, and K. Kim, "Sensors technologies for human activity analysis based on svm optimized by pso algorithm," in *2019 International Conference on Applied and Engineering Mathematics (ICAEM)*, 2019, pp. 145–150. DOI: 10.1109/ICAEM.2019.8853770.

[7] D. N. Tran and D. D. Phan, "Human activities recognition in android smartphone using support vector machine," in *2016 7th International Conference on Intelligent Systems, Modelling and Simulation (ISMS)*, 2016, pp. 64–68. DOI: 10.1109/ISMS.2016.51.

[8] L. C. Jatoba, U. Grossmann, C. Kunze, J. Ottenbacher, and W. Stork, "Context-aware mobile health monitoring: Evaluation of different pattern recognition methods for classification of physical activity," in *2008 30th Annual International Conference of the IEEE Engineering in Medicine and Biology Society*, 2008, pp. 5250–5253. DOI: 10.1109/IEMBS.2008.4650398.

[9] A. Nadeem, M. Hussain, O. Khan, A. Salam, S. Iqbal, and K. Ahsan, "Application specific study, analysis and classification of body area wireless sensor network applications," *Computer Networks*, vol. 83, 2015. DOI: 10.1016/j.comnet.2015.03.002.

[10] N. G. Paterakis, E. Mocanu, M. Gibescu, B. Stappers, and W. van Alst, "Deep learning versus traditional machine learning methods for aggregated energy demand prediction," in *2017 IEEE PES Innovative Smart Grid Technologies Conference Europe (ISGT-Europe)*, 2017, pp. 1–6. DOI: 10.1109/ISGTEurope.2017.8260289.

[11] A. K. M. Masum, M. E. Hossain, A. Humayra, S. Islam, A. Barua, and G. R. Alam, "A statistical and deep learning approach for human activity recognition," in *2019 3rd International Conference on Trends in Electronics and Informatics (ICOEI)*, 2019, pp. 1332–1337. DOI: 10.1109/ICOEI.2019.8862610.

[12] T. Huynh-The, C.-H. Hua, N. A. Tu, and D.-S. Kim, "Physical activity recognition with statistical-deep fusion model using multiple sensory data for smart health," *IEEE Internet of Things Journal*, vol. 8, no. 3, pp. 1533–1543, 2021. DOI: 10.1109/JIOT.2020.3013272.

[13] M. Hassan, M. Z. Uddin, A. Mohamed, and A. Almogren, "A robust human activity recognition system using smartphone sensors and deep learning," *Future Generation Computer Systems*, vol. 81, Nov. 2017. DOI: 10.1016/j.future.2017.11.029.

[14] B. Bamne, N. Shrivastava, L. Parashar, and U. Singh, "Transfer learning-based object detection by using convolutional neural networks," in *2020 International Conference on Electronics and Sustainable Communication Systems (ICESC)*, 2020, pp. 328–332. DOI: 10.1109/ICESC48915.2020.9156060.

[15] M. Nalini and K. Radhika, "Comparative analysis of deep network models through transfer learning," in *2020 Fourth International Conference on I-SMAC (IoT in Social, Mobile, Analytics and Cloud) (I-SMAC)*, 2020, pp. 1007–1012. DOI: 10.1109/I-SMAC49090.2020.9243469.

[16] C. Iorga and V.-E. Neagoe, "A deep cnn approach with transfer learning for image recognition," in *2019 11th International Conference on Electronics, Computers and Artificial Intelligence (ECAI)*, 2019, pp. 1–6. DOI: 10.1109/ECAI46879.2019.9042173.

[17] T. Sztyler and H. Stuckenschmidt, "On-body localization of wearable devices: An investigation of position-aware activity recognition," in *2016 IEEE International Conference on Pervasive Computing and Communications (PerCom)*, (Sydney, Australia, Mar. 14–18, 2016), http://ieeexplore.ieee.org/xpl/articleDetails.jsp?arnumber=7456521, IEEE Computer Society, 2016, pp. 1–9. DOI: 10.1109/PERCOM.2016.7456521.

[18] X. Qian, H. Chen, H. Jiang, J. Green, H. Cheng, and M.-C. Huang, "Wearable computing with distributed deep learning hierarchy: A study of fall detection," *IEEE Sensors Journal*, vol. 20, no. 16, pp. 9408–9416, 2020. DOI: 10.1109/JSEN.2020.2988667.

[19] L. Xu, J. Wang, X. Li, F. Cai, Y. Tao, and T. A. Gulliver, "Performance analysis and prediction for mobile internet of things (iot) networks: A cnn approach," *IEEE Internet of Things Journal*, pp. 1–1, 2021. DOI: 10.1109/JIOT.2021.3065368.

[20] M. Zeng, L. T. Nguyen, B. Yu, O. J. Mengshoel, J. Zhu, P. Wu, and J. Zhang, "Convolutional neural networks for human activity recognition using mobile sensors," in *6th International Conference on Mobile Computing, Applications and Services*, 2014, pp. 197–205. DOI: 10.4108/icst.mobicase.2014.257786.

[21] A. Juneja and N. N. Das, "Big data quality framework: Pre-processing data in weather monitoring application," in *2019 International Conference on Machine Learning, Big Data, Cloud and Parallel Computing (COMITCon)*, 2019, pp. 559–563. DOI: 10.1109/COMITCon.2019.8862267.

[22] V. D. R. Seethi and P. Bharti, "Cnn-based speed detection algorithm for walking and running using wrist-worn wearable sensors," in *2020 IEEE International Conference on Smart Computing (SMARTCOMP)*, 2020, pp. 278–283. DOI: 10.1109/SMARTCOMP50058.2020.00064.

[23] H. Cho and S. M. Yoon, "Divide and conquer-based 1d cnn human activity recognition using test data sharpening," *Sensors*, vol. 18, no. 4, 2018, Last accessed: 6/7/2021, ISSN: 1424-8220. DOI: 10.3390/s18041055. [Online]. Available: https://www.mdpi.com/1424-8220/18/4/1055.

[24] N. Srivastava, G. Hinton, A. Krizhevsky, I. Sutskever, and R. Salakhutdinov, "Dropout: A simple way to prevent neural networks from overfitting," *Journal of Machine Learning Research*, vol. 15, pp. 1929–1958, Jun. 2014.

[25] S. Lym, D. Lee, M. O'Connor, N. Chatterjee, and M. Erez, "Delta: Gpu performance model for deep learning applications with in-depth memory system traffic analysis," in *2019 IEEE International Symposium on Performance Analysis of Systems and Software (ISPASS)*, 2019, pp. 293–303. DOI: 10.1109/ISPASS.2019.00041.

[26] C. Goutte and E. Gaussier, "A probabilistic interpretation of precision, recall and f-score, with implication for evaluation," vol. 3408, Apr. 2005, pp. 345–359, ISBN: 978-3-540-25295-5. DOI: 10.1007/978-3-540-31865-1_25.

[27] D. Yun, W. Liu, C. Q. Wu, N. S. Rao, and R. Kettimuthu, "Performance prediction of big data transfer through experimental analysis and machine learning," in *2020 IFIP Networking Conference (Networking)*, 2020, pp. 181–189.

[28] W. Sun and X. Qian, "An improved transfer learning algorithm for document categorization based on data sets reconstruction," in *Proceedings of the 10th World Congress on Intelligent Control and Automation*, 2012, pp. 575–578. DOI: 10.1109/WCICA.2012.6357945.

[29] K. R. Weiss and T. M. Khoshgoftaar, "Comparing transfer learning and traditional learning under domain class imbalance," in *2017 16th IEEE International Conference on Machine Learning and Applications (ICMLA)*, 2017, pp. 337–343. DOI: 10.1109/ICMLA.2017.0-138.

[30] H. Mizuno, H. Nagai, K. Sasaki, H. Hosaka, C. Sugimoto, K. Khalil, and S. Tatsuta, "Wearable sensor system for human behavior recognition (first report: Basic architecture and behavior prediction method)," in *TRANSDUCERS 2007 - 2007 International Solid-State Sensors, Actuators and Microsystems Conference*, 2007, pp. 435–438. DOI: 10.1109/SENSOR.2007.4300161.

[31] J. Zhang, "Deep transfer learning via restricted boltzmann machine for document classification," in *2011 10th International Conference on Machine Learning and Applications and Workshops*, vol. 1, 2011, pp. 323–326. DOI: 10.1109/ICMLA.2011.51.

[32] M. Monshizadeh, V. Khatri, B. G. Atli, R. Kantola, and Z. Yan, "Performance evaluation of a combined anomaly detection platform," *IEEE Access*, vol. 7, pp. 100 964–100 978, 2019. DOI: 10.1109/ACCESS.2019.2930832.

[33] L. Verde, G. De Pietro, A. Ghoneim, M. Alrashoud, K. N. Al-Mutib, and G. Sannino, "Exploring the use of artificial intelligence techniques to detect the presence of coronavirus covid-19 through speech and voice analysis," *IEEE Access*, vol. 9, pp. 65 750–65 757, 2021. DOI: 10.1109/ACCESS.2021.3075571.

[34] Z. Fu, X. He, E. Wang, J. Huo, J. Huang, and D. Wu, "Personalized human activity recognition based on integrated wearable sensor and transfer learning," *Sensors*, vol. 21, p. 885, Jan. 2021. DOI: 10.3390/s21030885.

[35] Y. Zhang, J. Li, Y. Guo, C. Xu, J. Bao, and Y. Song, "Vehicle driving behavior recognition based on multi-view convolutional neural network with joint data augmentation," *IEEE Transactions on Vehicular Technology*, vol. 68, no. 5, pp. 4223–4234, 2019. DOI: 10.1109/TVT.2019.2903110.